

## Article

# Biodiesel Production through *Rhodotorula toruloides* Lipids and Utilization of De-Oiled Biomass for Congo Red Removal

Mohammed S. Almuhayawi <sup>1</sup>, Elhagag A. Hassan <sup>2,\*</sup>, Saad Almasaudi <sup>3</sup>, Nidal Zabermaawi <sup>3</sup>,  
Esam I. Azhar <sup>4,5</sup>, Azhar Najjar <sup>3</sup>, Khalil Alkuwaity <sup>4</sup>, Turki S. Abujamel <sup>5,6</sup>, Turki Alamri <sup>7</sup>,  
and Steve Harakeh <sup>8,9,\*</sup>

- <sup>1</sup> Department of Clinical Microbiology and Immunology, King Abdulaziz University, Jeddah 21589, Saudi Arabia; msalmuhayawi@kau.edu.sa
- <sup>2</sup> Department of Botany and Microbiology, Faculty of Science, Assiut University, Assiut 71516, Egypt
- <sup>3</sup> Department of Biological Sciences, Faculty of Science, King Abdulaziz University, Jeddah 21589, Saudi Arabia; smasaudi@kau.edu.sa (S.A.); nzabermaawi@kau.edu.sa (N.Z.); anajjar@kau.edu.sa (A.N.)
- <sup>4</sup> Department of Medical Laboratory Sciences, Faculty of Applied Medical Sciences, King Abdulaziz University, Jeddah 21589, Saudi Arabia; eazhar@kau.edu.sa (E.I.A.); kalkuwaity@kau.edu.sa (K.A.)
- <sup>5</sup> Special Infectious Agents Unit—BSL3, King Fahd Medical Research Center, King Abdulaziz University, Jeddah 21589, Saudi Arabia; tabujamel@kau.edu.sa
- <sup>6</sup> Vaccines and Immunotherapy Unit, King Fahd Medical Research Center, King Abdulaziz University, Jeddah 21589, Saudi Arabia
- <sup>7</sup> Family and Community Medicine Department, Faculty of Medicine in Rabigh, King Abdulaziz University, Jeddah 21589, Saudi Arabia; olbalamri7@kau.edu.sa
- <sup>8</sup> King Fahd Medical Research Center, King Abdulaziz University, Jeddah 21589, Saudi Arabia
- <sup>9</sup> Yousef Abdul Latif Jameel Scientific Chair of Prophetic Medicine Application, Faculty of Medicine, King Abdulaziz University, Jeddah 21589, Saudi Arabia
- \* Correspondence: elhagaghassan@aun.edu.eg (E.A.H.); sharakeh@gmail.com (S.H.)



**Citation:** Almuhayawi, M.S.; Hassan, E.A.; Almasaudi, S.; Zabermaawi, N.; Azhar, E.I.; Najjar, A.; Alkuwaity, K.; Abujamel, T.S.; Alamri, T.; Harakeh, S. Biodiesel Production through *Rhodotorula toruloides* Lipids and Utilization of De-Oiled Biomass for Congo Red Removal. *Sustainability* **2023**, *15*, 13412. <https://doi.org/10.3390/su151813412>

Academic Editor: Domenico Licursi

Received: 30 June 2023

Revised: 29 August 2023

Accepted: 31 August 2023

Published: 7 September 2023



**Copyright:** © 2023 by the authors. Licensee MDPI, Basel, Switzerland. This article is an open access article distributed under the terms and conditions of the Creative Commons Attribution (CC BY) license (<https://creativecommons.org/licenses/by/4.0/>).

**Abstract:** The current study aimed to investigate the potentiality of yeast isolate *Rhodotorula toruloides* Y1124 to be used as a feedstock for biodiesel production, and the reutilization of the de-oiled yeast biomass wastes as a biosorbent for the biosorption of Congo red from aquatic solutions was investigated. From screening results, eight yeast isolates were referred to as oleaginous microorganisms, of which yeast isolate *Rhodotorula toruloides* Y1124 was the highest lipid-accumulating isolate and was used as a feedstock for biodiesel production. The highest lipid accumulation (64.8%) was significantly dependent on the glucose concentration, pH, and incubation temperature according to Plackett–Burman and central composite design results. Under optimized conditions, the estimated amount of biodiesel synthesis from *Rhodotorula toruloides* biomass represented 82.12% of total analytes. The most prevalent fatty acid methyl esters were hexadecanoic and 11-octadecenoic, comprising 30.04 and 39.36% of total methyl esters which were compatible with plant oils. The optimum biosorption conditions for Congo red removal were pH 6, a 15 min contact time, and an initial dye concentration of 40 mg L<sup>-1</sup>. The biosorption isothermal and kinetics fitted well with the Langmuir model and the maximal biosorption capacity (q<sub>max</sub>) was 81.697 mg g<sup>-1</sup>. Therefore, the current study may offer a sustainable feedstock with potential viability for both the synthesis of biodiesel and the removal of organic dyes.

**Keywords:** oleaginous yeast; *Rhodotorula toruloides*; biosorption; central composite design; single cell oil; transesterification/esterification processes

## 1. Introduction

Fossil fuels are the main source of energy for motorization, industrialization, and economic growth worldwide. Nowadays, humans face many issues concerning the global ongoing use of petroleum energies because climate change has resulted from global warming and environmental air pollution. Based on the rate of production versus consumption,

petroleum reserves will last for at least 100 years and probably more [1]. Because of the increase in petroleum-based fuel prices and their adverse effects on the environment, alternative methods have been sought. Such alternative biofuel technology development with the aim to improve the strategies that generate eco-friendly and sustainable energy sources from renewable materials is required urgently [2]. Thus, bioenergy production using microbial fermentation from renewable feedstock is considered a prospective alternative energy source [3–5]. Biodiesel is the esters of fatty acids generated from renewable sources such as edible/non-edible oils or animal fats by transesterification/esterification processes of triglycerides or free fatty acids [6,7]. Biodiesel is considered an excellent alternative fuel to conventional petroleum diesel owing to its biodegradability and nontoxicity [8,9]. In addition, the raw material is a critical consideration in the biodiesel industry because the cost of biodiesel is influenced mainly by the processed raw material utilized. Feedstock now accounts for more than 80% of the expenditures associated with biodiesel manufacturing [10]. Around 95% of global biodiesel output is derived from edible oils, which is considered to be wasteful due to the world's food crisis [11]. As a result, the latest trend is to produce biodiesel from inexpensive non-edible oil [12]. Because of their high triglyceride content, various feedstocks, such as palm, jatropha, microorganisms, tallow coconut insect fats, wet spent coffee grounds, *Melia azedarach* and *Ricinus communis*, and waste cooking oil, have a high productivity in biodiesel manufacturing [13–16]. Microbial lipids from microorganisms are considered as a prospective feedstock to improve the world bio-oil production for biodiesel synthesis that would cause safe ecosystem impacts [17]. Oleaginous yeast appears to be one of the potent feedstocks for renewable biodiesel generation that is capable of meeting the global demand for transport fuels. Oleaginous yeast has the ability to produce lipids with more than 20% of their dry biomass and it does so more efficiently than other microbes. This is because of its high rate of productivity; there is no need for land cultivation and it can grow on various organic wastes with a high growth rate [18], so making oleaginous yeast is considered a promising feedstock for biodiesel production which is economically competitive with petro-diesel. But, biodiesel commercialization and popularity are restricted by its use in cold climates and prolonged storage because of its poor low-temperature viscosity and oxidation stability, which depend mainly on the physico-chemical characteristics of biodiesel attributed to the fatty acids content of the oil feedstock [19]. As well being used to increase the feasibility of oleaginous yeast, the residual de-oiled yeast biomass that remains after biodiesel production [20] can be reutilized and recycled as a good biosorbent agent for anthropogenic dye pollutants in aquatic ecosystems [21].

Freshwater systems have significant ecological roles, including as reservoirs of organic carbon and in fulfilling human life requirements, including providing the resource of drinking water and being used for industrial and agricultural purposes. However, due to the sharp increase in the world's human population, accelerating urbanization, industrialization, and pollution from anthropogenic sources, natural inland waters have undergone significant change, with detrimental consequences for both aquatic ecosystems and people [22,23]. Thus, these organic pollutants produced from many industries are creating rising alarms and gaining great importance [24–26]. Synthetic dyes are considered one of the most common pollutants that are discharged as effluents into freshwater and other aquatic ecosystems from different industries such as textile and cloth dyeing, paper manufacturing, printing, color photography, food products, pharmaceuticals, and cosmetics [27]. Annually, about 800,000 tons of synthetic dyes are produced (50% azo dyes) [28], and approximately 10–15% of these dyes are discharged into aquatic ecosystems and cause an undeniable environmental problem due to their stability against light, temperature, and biodegradation [29]. Consequently, these synthetic dyes are considered toxic and highly persistent emerging pollutants in nature, which can cause adverse impacts on human and animals' health [30], such as teratogenesis, carcinogenesis, and mutagenesis [31]. Congo red (CR) is one of the most common industrial dyes that have a complex aromatic anionic azo dye that exhibits a hindrance to photo and chemical oxidation as well as biodegra-

dation [32]. Therefore, how to effectively get rid of these dyes from aquatic systems has become a pressing and urgent issue. Various strategies have been applied for the removal of these dyes, including photodegradation, chemical oxidation, microbial degradation, and membrane- and nanofiltration [32,33]. Conspicuously, the adsorption process by microbial biomasses has been emphasized as a promising feasible technology for the treatment of dye-containing effluents [34]. Consequently, the current study aimed to evaluate the possible role of oleaginous yeast *Rhodotorula toruloides* Y1124 as a feedstock for biodiesel generation and optimize the culture and environmental conditions using Plackett–Burman design (PBD) and central composite design (CCD) for the highest accumulation of single cell oils for efficient biodiesel production. Furthermore, subsequent to lipid extraction for biodiesel production the de-oiled yeast biomasses were utilized for the biosorption of Congo red through studying the factors affecting the biosorption process, as well the isotherm and mechanism of the biosorption. This approach may increase the economic applicability of biodiesel production through subsequent reutilization of produced de-oiled yeast biomass for wastewater treatment.

## 2. Materials and Methods

### 2.1. Isolation for Yeast Isolates

Yeasts were isolated from 25 sugary wastewater samples collected from Assiut governorate, Egypt, on yeast malt extract agar (YMA) medium containing 10 g L<sup>-1</sup> glucose, 3 g L<sup>-1</sup> yeast extract, 5 g L<sup>-1</sup> peptone, 3 g L<sup>-1</sup> malt extract, 0.25 g L<sup>-1</sup> chloramphenicol, and 18 g L<sup>-1</sup> agar. The sugary wastewater samples were streaked onto sterilized plates containing YMA and incubated at 28 ± 2 °C for 4 days. After the incubation period, the resulting colonies with varying culture morphologies were picked, purified, and examined under the light microscope. The isolated yeasts were maintained in Yeast malt agar (YMA) medium at 4 °C for screening the lipid accumulation potential.

### 2.2. Screening for Lipid Accumulation by Oleaginous Yeast

The tested yeast isolates were collected and blended in sterilized distilled H<sub>2</sub>O. One milliliter of the yeast suspension (1 × 10<sup>5</sup> cell mL<sup>-1</sup>) was used for inoculation of the culture medium for lipid production. The tested yeasts were grown in 250-mL conical flasks containing 100 mL sterilized culture medium containing 30 g L<sup>-1</sup> glucose; 2 g L<sup>-1</sup> (NH<sub>4</sub>)<sub>2</sub>SO<sub>4</sub>; 1 g L<sup>-1</sup> KH<sub>2</sub>PO<sub>4</sub>; 1 g L<sup>-1</sup> MgSO<sub>4</sub> 7H<sub>2</sub>O; 1 g L<sup>-1</sup> CaCl<sub>2</sub> 2H<sub>2</sub>O; 1 g L<sup>-1</sup> NaCl; 0.5 g L<sup>-1</sup> yeast extract and 0.25 g L<sup>-1</sup> chloramphenicol. Then the culture was incubated at 28 ± 1 °C for 7 days in an orbital shaker at 120 rpm, then yeast biomasses were collected by centrifugation at 6000 rpm and then dried overnight at 50 °C. The dried cells were weighed for dry weight determination and three replicates were used independently. Single-cell oils (Lipids) were extracted using chloroform methanol (2:1) procedure [35], then the lipid content was assayed colorimetrically by the phospho-vanillin reagent method [36]. All the experiments were conducted in triplicate. The highest-lipid-accumulating yeast isolate was identified based on the phenotypic (colony color, cell shape, and bud and pseudohyphae formation), with the aid of optical microscope Olympus CX41, as well as the biochemical characteristics, including urease test, nitrate reductase reaction, indole production, and utilization of different carbon sources, e.g., soluble starch, glucose, xylose, sucrose, galactose, lactose and maltose [37,38]. The selected oleaginous yeast was grown on YMA plates for 4 days at 28 ± 1 °C and preserved in the mycological herbarium, Department of Botany and Microbiology, Faculty of Science, Assiut University.

### 2.3. Enhancement of Lipid Accumulation by Oleaginous Yeast

The impact of nutritional and environmental variables on lipid accumulation by the oleaginous yeast was investigated using two models, Plackett–Burman design (PBD) and central composite design (CCD), using Design-Expert software to assay the significance of the individual variables and their interactions on lipid accumulation by the oleaginous yeast (Table 1). Seven independent nutritional and environmental variables were assayed

at a high level (+1) and low level (−1) for enhancement of lipid accumulation by oleaginous yeast (Table 1). Collectively, the nutritional and environmental variables effects on lipid accumulation by the oleaginous yeast were assayed using Plackett–Burman design (PBD) in 12 experiments and central composite design (CCD) design in 50 experiments (as shown in Tables S1 and S2), and all experiments were conducted in three replicates.

**Table 1.** Levels of the tested parameters for lipid accumulation by *Rhodotorula toruloides*.

Factor Code	Tested Factor	Unit	Level	
			Low (−1)	High (+1)
A	Glucose	g L <sup>−1</sup>	25	35
B	(NH <sub>4</sub> ) <sub>2</sub> SO <sub>4</sub>	g L <sup>−1</sup>	1.50	2.50
C	KH <sub>2</sub> PO <sub>4</sub>	g L <sup>−1</sup>	0.50	1.50
D	Yeast extract	g L <sup>−1</sup>	0.25	0.75
E	Temperature	°C	25	35
F	pH		6	8
G	Incubation period	Days	3	5

For each tested run, the content of lipids was recorded as responses and the obtained results were analyzed by multiple regression to correlate each response to the tested variable. The PBD model was illustrated by the following equation (Equation (1)):

$$\text{Total lipid (\%)} = \beta_0 + \sum \beta_i X_i + \sum \beta_{ij} X_i X_j + \sum \beta_{ii} X_i^2 \quad (1)$$

where  $\beta_0$  is the model regression coefficient;  $X_i$  and  $X_j$  are the levels of tested variable;  $\beta_i$  is the linear coefficient;  $\beta_{ij}$  is the interaction coefficient; and  $\beta_{ii}$  is the quadratic coefficient.

The obtained experimental results were statistically analyzed by ANOVA to define the significance of the model ( $p \leq 0.05$ ) and in response to different tested conditions. The responses were plotted in suitable graphs using Design-Expert software version 11.1.2.0 (Stat-Ease Inc., Minneapolis, MN, USA).

#### 2.4. Biodiesel Production from Microbial Lipids Chemically

Biodiesel production from the extracted lipids from oleaginous yeast was conducted by the transesterification method, as reported by Vicente et al. [39]. The transesterification reaction was conducted in 10 mL stopper glass vials containing 0.1 mL extracted lipid, 4 mL methanol, 1 mL HCl, and 1 mL chloroform. The mixture was incubated at 70 °C overnight under shaking conditions; then, 1 mL n-hexane was mixed under vortex to extract the produced biodiesel (top layer) as fatty acid methyl esters (FAMES). A total of 2  $\mu$ L of FAMES was analyzed by GC/MS (Model: DPC-Direct Probe Controller (DPC-20451), Thermo Scientific, Waltham, MA, USA) at the Chemistry Department, Faculty of Science, Assiut University. GC/MS was equipped with a capillary column TG-5MS (30 m, 0.25 mm i.d., 1  $\mu$ m film thicknesses). The oven temperature was 80 °C for 5 min, then the temperature was increased at the rate of 10 °C min<sup>−1</sup> to 150 °C and 200 °C for 10 min each, and finally, the oven temperature was raised at an increasing rate of 5 °C min<sup>−1</sup> to 250 °C for 13 min. The injector temperature was 250 °C and the detector temperature was 300 °C. The percent of FAMES yield was estimated by comparison with the peak area of internal standards at the specific retention time [40].

#### 2.5. Determination of the Quality of Biodiesel

The quality of the produced biodiesel was evaluated based on physicochemical characteristics of FAMES (biodiesel) using the following mathematical equations: The calculated values were compared with the EU biodiesel standard EN 14214 and US biodiesel standard specification ASTM D6751.

$$\text{Density}(p) = \sum (c_i \times \rho_i) \quad (2)$$

where  $c_i$  indicates the concentration (mass fraction);  $\rho_i$  = the density of component (individual the fatty acid methyl ester) present in the biodiesel.

$$\text{Kinematicviscosity } (\nu_{\text{mix}}) = \sum (A_c \times \nu_c) \quad (3)$$

where  $\nu_{\text{mix}}$  indicates the kinematic viscosity of the fatty acid methyl esters produced,  $A_c$  indicates the relative amount of the each ester in biodiesel sample (as obtained by GC/MS), and  $\nu_c$  obtained from the kinematic viscosity database of each fatty acid methyl ester (FAME).

$$\text{SaponificationNumber (SN)} = \sum (254 \times A_i) / MW_i \quad (4)$$

where  $A_i$  indicates the percentage of each FAME obtained by GC/MS and  $MW_i$  indicates the molecular weight of (FAME).

$$\text{IodineValue (IV)} = \sum (254 \times D \times A_i) / MW_i \quad (5)$$

where  $D$  indicates the number of the double bonds.

$$\text{HigherHeatingValue (HHV)} = 49.43 - [0.041(\text{SN}) + 0.015(\text{IV})] \quad (6)$$

$$\text{CetaneNumber (CN)} = 1.068 \sum (\text{CN}_i \times W_i) - 6.747 \quad (7)$$

where  $\text{CN}_i$  indicates the reported CN of pure FAME available in the database;  $W_i$  indicates the mass fraction of the each FAME quantified by GC/MS.

## 2.6. Biosorption Isotherms of Congo Red Using De-Oiled Biomass Wastes

### 2.6.1. Preparation of De-Oiled Yeast Biomasses as a Biosorbent

After lipid extraction from yeast biomass, sterile distilled water was used three times to rinse the waste yeast biomass, and then dried overnight and used as a biosorbent material for Congo red.

### 2.6.2. Effect of Contact Time on the Biosorption Efficiency of Congo Red by Dried De-Oiled Yeast Biomasses

Fifty mg of dried de-oiled cells were mixed with 50 mL of Congo red solution ( $50 \text{ mg L}^{-1}$ ). The dried de-oiled cells/dye mixtures were agitated at 150 rpm at  $28 \pm 2 \text{ }^\circ\text{C}$ . The pH value of the initial solution was adjusted to 7.0. Samples from the solutions were obtained at the predetermined time intervals (0–60 min) and centrifuged for 5 min at 8000 rpm. Using a spectrophotometer at a wavelength of 488 nm, the amount of Congo red present in the resultant supernatant was measured.

### 2.6.3. Effect of pH on Biosorption Efficiency of Congo Red by De-Oiled Yeast Biomasses

Using dried, de-oiled cells with 20 mL of dye solution and varied pH values (range from 1.0 to 7.0) at  $28 \pm 2 \text{ }^\circ\text{C}$ , the impact of solution pH on Congo red biosorption was examined. By adding either 0.1 M NaOH or 0.1 M HCl, the pH was adjusted.

## 2.7. Biosorption Isotherms of Congo Red by De-Oiled Yeast Biomasses

The Congo red biosorption isotherm studies used Langmuir isotherm, which describes the state of equilibrium between an adsorbate and an adsorbent system, when the adsorbate is restricted to one molecular layer when or before a relative pressure of unity is attained. The isotherm experiment was evaluated using 20 mg of the biosorbent agent (dry de-oiled cells) and various quantities of Congo red were used in 20 mL of deionized water at pH 6.0. The tubes with the mixtures were agitated at 150 rpm for 30 min at  $28 \pm 2 \text{ }^\circ\text{C}$ . The tubes were then centrifuged for 5 min at 8000 rpm, and the supernatant was examined using a spectrophotometer to determine the amount of dye that was remaining.

### 2.8. Congo Red Biosorption Evolution

Congo red biosorption was calculated using the following equation (Equation (8)):

$$\text{Congoredremoval}(\%) = \frac{(C_0 - C_i)}{C_0} \times 100 \quad (8)$$

where  $C_0$  is dye initial concentration and  $C_i$  is dye equilibrium concentration.

### 2.9. Fourier-Transform Infrared Spectroscopy (FTIR) Analysis of Deoiled Yeast Biomass

The functional groups of de-oiled yeast biomasses were examined using FTIR spectrometer using the KBr pressed disk procedure (Thermo Scientific Nicolet iS10 FT-IR Spectrometer, Waltham, MA, USA) at the Chemistry Department, Faculty of Science, Assiut University.

## 3. Results

### 3.1. Isolation and Screening for Lipid Accumulation by Isolated Yeast Isolates

The obtained data in Table 2 revealed that, out of 13 yeast isolates recovered from sugary water samples, 8 yeast isolates were oleaginous microorganisms (producing more than 20% total lipid) with various degrees of lipid accumulation. The highest lipid production was recorded for yeast isolate Y1124, with 47.83%.

**Table 2.** Lipid accumulation (%) and dry biomass ( $\text{g L}^{-1}$ ) of tested yeast isolates.

Test	Yeast Isolates	Total Lipids %	Yeast Dry Biomass ( $\text{g L}^{-1}$ )
	Y1110	29.14 ± 2.16	6.82 ± 0.52
	Y1118	35.02 ± 1.96	4.73 ± 1.14
	Y1119	14.91 ± 0.96	5.71 ± 0.83
	Y1120	18.16 ± 1.14	9.06 ± 0.72
	Y1124	47.83 ± 1.37	7.80 ± 1.50
	Y1133	30.42 ± 2.05	5.62 ± 0.94
	Y1136	21.07 ± 1.46	8.04 ± 0.92
	Y1201	16.72 ± 1.53	7.94 ± 1.05
	Y1204	26.55 ± 0.88	4.95 ± 0.47
	Y1205	19.03 ± 0.70	8.13 ± 0.68
	Y1206	41.43 ± 1.85	5.92 ± 1.21
	Y1208	39.85 ± 1.09	7.05 ± 0.90
	Y1210	13.28 ± 0.64	4.22 ± 1.83

The highest lipid accumulating yeast isolate Y1124 was identified using phenotypic and biochemical characterization as *Rhodotorula toruloides*. From the obtained results of characterization, yeast isolate *Rhodotorula toruloides* is characterized by pink-colored growth; the yeast cells showed budding formation, and globose to subglobose cells and simple pseudohyphae may be present (Table 3). In addition, yeast isolate exhibited positive reactions for glucose, xylose, sucrose, galactose, maltose, and urease production, but negative results are exhibited for nitrate reductase and indole production. The obtained data revealed that yeast isolate *Rhodotorula toruloides* Y1124 exhibited high lipid content. Consequently, the optimization of lipid accumulation using the yeast isolate *Rhodotorula toruloides* Y1124 using central composite design was performed in order to maximize the lipid accumulation capability for biodiesel production. Then, the de-oiled yeast wastes that remained after lipid extraction (biowaste) were utilized as a biosorbent for the removal of toxic Congo red dyes from aquatic solutions to maximize the applicability of yeast biomasses.

**Table 3.** Morphological and physiological characteristics of the isolated pathogenic bacterial isolate.

Parameter	Result
Phenotypic Characteristics	
Colony color	Pink colored
Shape	Globose to subglobose cells
Budding	Present
Pseudohyphae	May be present
Biochemical reactions	
Urease test	+
Nitrate reductase	–
Indole production	–
Soluble starch	–
Glucose	+
Xylose	+
Sucrose	+
Galactose	+
Lactose	–
Maltose	+

### 3.2. Optimization of Lipid Accumulation by Oleaginous Yeast

In the current study, the effects of various nutritional and environmental parameters were assayed on lipid accumulation potential by oleaginous yeast. Making predictions about the response for specific levels of each variable is possible using the equation in terms of coded variables. By design, the factors' high levels are coded as +1 and their low levels as –1. By comparing the variable coefficients, the coded equation can be used to determine the relative importance of the components. The obtained data stated that the tested variables showed different impacts on lipid accumulation by oleaginous yeast. The partograph showed the significance of each tested variable on lipid accumulation by oleaginous yeast. Glucose,  $\text{KH}_2\text{PO}_4$ , yeast extract and temperatures showed positive effects on lipid accumulation (Figure 1). The analysis of variance (ANOVA) of the obtained results exhibited that the model F-value was significant, being 111.84, and there is only a 0.01% chance that an F-value this large could occur due to noise (Table 4). The Predicted  $R^2$  of 0.9579 is in reasonable agreement with the Adjusted  $R^2$  of 0.9805; i.e., the difference is less than 0.2. In addition,  $p$ -values less than 0.0500 revealed that model terms are significant. In this case, the tested variables, glucose, temperature, and interacted ammonium sulphate, are significant model terms. Values greater than 0.1000 indicate the model terms are not significant. The Box-Cox plot revealed the most powerful transformation; the Lambda value ( $\lambda$ ) = 1 and the ratio of maximum/minimum values was less than 3 (Figure 2). The ANOVA statistical analysis of CCD model revealed that only glucose concentration and initial pH among the tested variables were significant ( $p > 0.05$ ) as shown in Table 5. Furthermore, all the predicted responses of the model approximately fit experimental values, and this showed that the hypothesis that the total lipid model equation is suitable to explain the response of the experimental data of lipid accumulation. Furthermore, the results of lipid contents are calculated using the CCD model according to the resulting equation (Equation (9)):

$$\begin{aligned} \text{Total lipid (\%)} = & 38.158 + 4.39087 \times A + (-1.93281 \times B) + (-0.637376 \times C) + 0.309496 \times D + 0.23602 \times E + \\ & (-3.62029 \times F) + 1.21766 \times G + (-0.934549) \times AB + (-0.641551 \times AC) + 2.35899 \times AD + (-0.552248 \times AE) + \\ & 0.248359 \times AF + 0.441188 \times AG + (-1.0653 \times BF) + 0.33956 \times CF + 1.95705 \times DF + (-0.493953 \times EF) \\ & + (-1.80381 \times FG) \end{aligned} \quad (9)$$

The model is suggested to be significant by the model's F-value of 1.97.  $P$  Model terms are considered significant when the  $p$ -value is less than 0.0500. Thus, glucose and pH values are significant model terms. Model terms are not significant if the value is higher than 0.1000. The F-value for the lack of fit, 1.14, indicates that the lack of fit is not significant in comparison to the pure error. The most effective tested combined parameters (other

parameters were at zero coded units) on lipid accumulation by oleaginous yeast were presented in Figure 3. The obtained data revealed that the highest concentration of carbon source, glucose, led to the enhancement of lipid accumulation, as shown in Figure 3A,B. The highest lipid content was recorded at the lowest concentration of inorganic nitrogen source  $(\text{NH}_4)_2\text{SO}_4$  (Figure 3C,E). On the other hand, different concentrations of  $\text{KH}_2\text{PO}_4$  did not show obvious effects on lipid accumulation by oleaginous yeast (Figure 3D). In addition, the lipid content was increased by increasing yeast extract concentration and decreasing the initial pH value of the culture medium (Figure 3F). Furthermore, the lipid content was enhanced by increasing the incubation temperature and decreasing the initial pH value of the culture medium, as shown in Figure 3G. The highest lipid concentration was estimated with increasing the incubation period and decreasing pH value of the culture medium (Figure 3H). The optimum variables for the highest lipid accumulation (64.8%) by oleaginous yeast were  $38 \text{ g L}^{-1}$  glucose;  $2 \text{ g L}^{-1}$   $(\text{NH}_4)_2\text{SO}_4$ ;  $1 \text{ g L}^{-1}$   $\text{KH}_2\text{PO}_4$ ;  $0.5 \text{ g L}^{-1}$  yeast extract, and an initial pH value of 7 and incubated at  $30^\circ\text{C}$  for 4 days.

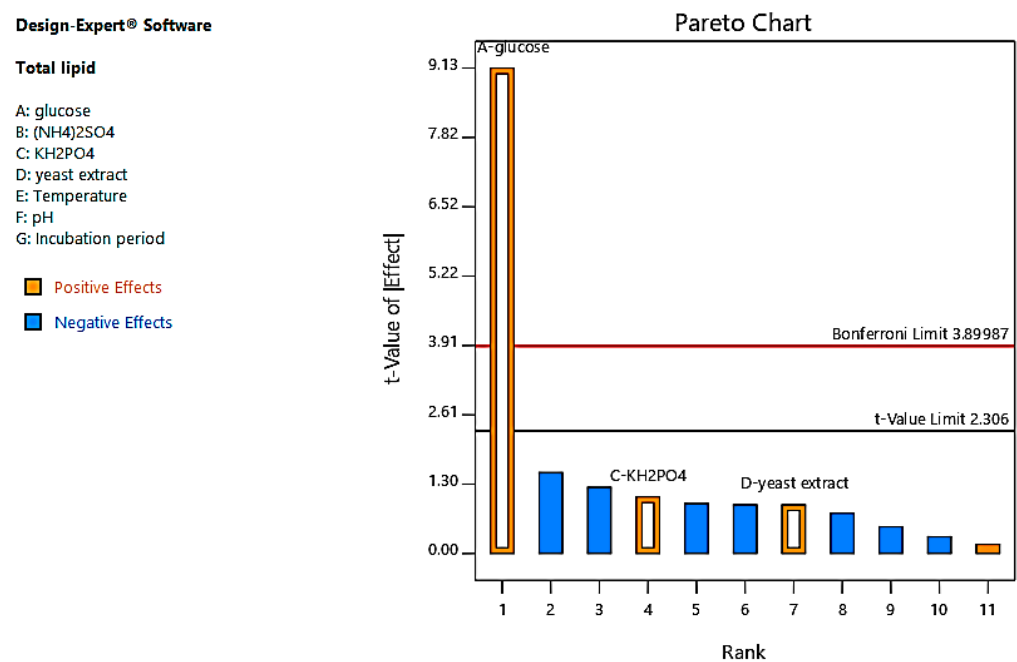


Figure 1. Pareto chart for total lipids accumulated by the oleaginous yeast.

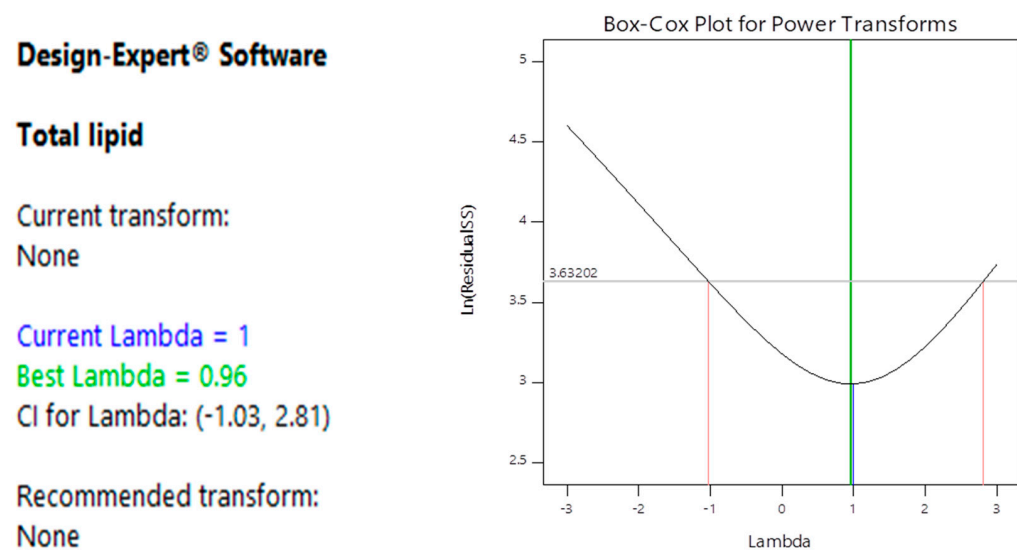


Figure 2. Box-Cox Plot for lipid accumulation obtained from PBD model.

**Table 4.** Analysis of variance (ANOVA) of the PDB results for lipid accumulation by oleaginous yeast.

Source	Sum of Squares	Df	Mean Square	F-Value	p-Value	
Model	1857.31	5	371.46	111.84	<0.0001	Significant
A—glucose	1349.70	1	1349.70	406.38	<0.0001	Significant
B-(NH <sub>4</sub> ) <sub>2</sub> SO <sub>4</sub>	11.56	1	11.56	3.48	0.1113	not significant
E—Temperature	58.09	1	58.09	17.49	0.0058	Significant
AB (glucose:(NH <sub>4</sub> ) <sub>2</sub> SO <sub>4</sub> )	120.15	1	120.15	36.18	0.0010	Significant
BE ((NH <sub>4</sub> ) <sub>2</sub> SO <sub>4</sub> : Temperature)	31.33	1	31.33	9.43	0.0219	Significant
Residual	19.93	6	3.32			
Cor Total	1877.24	11				

**Table 5.** ANOVA statistical analysis of the CCD results for lipid accumulation by oleaginous yeast.

Source	Sum of Squares	Df	Mean Square	F-Value	p-Value	Significance
Model	1655.89	18	91.99	1.9700	0.0471	Significant
A—Glucose	569.90	1	569.90	12.2100	0.0015	Significant
B—(NH <sub>4</sub> ) <sub>2</sub> SO <sub>4</sub>	106.35	1	106.35	2.2800	0.1413	not significant
C—KH <sub>2</sub> PO <sub>4</sub>	11.94	1	11.94	0.2557	0.6167	not significant
D—Yeast extract	2.73	1	2.73	0.0584	0.8106	not significant
E—Temperature	1.59	1	1.59	0.0340	0.8550	not significant
F—pH	385.06	1	385.06	8.2500	0.0073	Significant
G—Incubation period	42.21	1	42.21	0.9043	0.3490	not significant
AB (Glucose: (NH <sub>4</sub> ) <sub>2</sub> SO <sub>4</sub> )	20.97	1	20.97	0.4492	0.5077	not significant
AC (Glucose: KH <sub>2</sub> PO <sub>4</sub> )	9.89	1	9.89	0.2118	0.6486	not significant
AD (Glucose: yeast extract)	133.58	1	133.58	2.8600	0.1007	not significant
AE (Glucose: temperature)	7.32	1	7.32	0.1568	0.6948	not significant
AF (Glucose: pH)	1.48	1	1.48	0.0317	0.8597	not significant
AG (Glucose: incubation period)	4.67	1	4.67	0.1001	0.7538	not significant
BF ((NH <sub>4</sub> ) <sub>2</sub> SO <sub>4</sub> : pH)	28.28	1	28.28	0.6058	0.4423	not significant
CF (KH <sub>2</sub> PO <sub>4</sub> : pH)	3.10	1	3.10	0.0665	0.7983	not significant
DF (yeast extract: pH)	98.99	1	98.99	2.1200	0.1554	not significant
EF (temperature: pH)	6.31	1	6.31	0.1351	0.7157	not significant
FG (pH: incubation period)	81.07	1	81.07	1.7400	0.1972	not significant
Residual	1446.94	31	46.68			
Lack of fit	1237.77	26	47.61	1.1400	0.4909	not significant
Pure error	209.17	5	41.83			
Cor Total	3102.83	49				

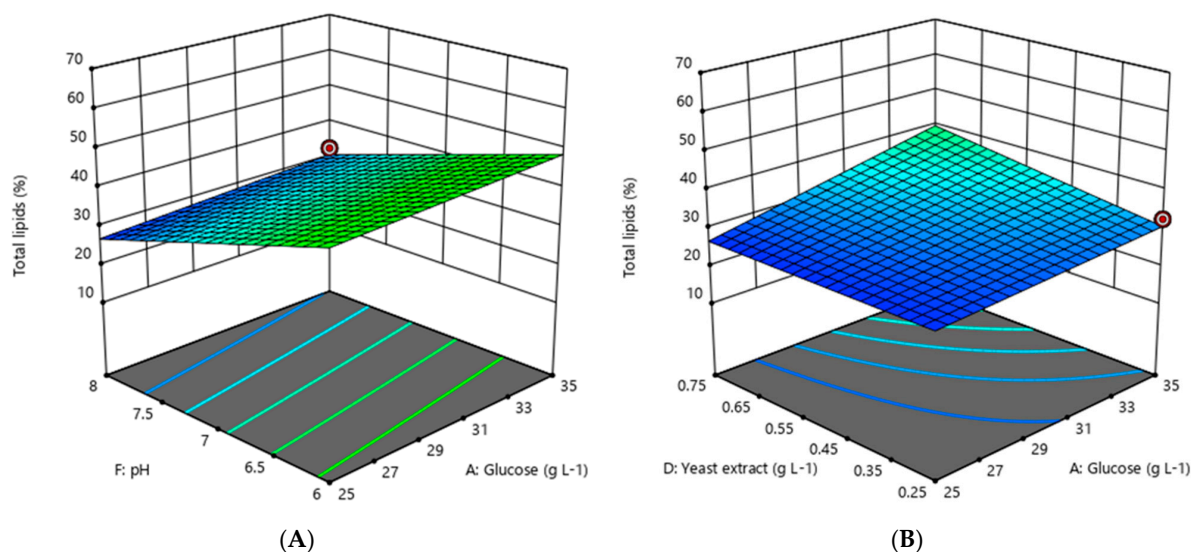


**Figure 3.** Cont.

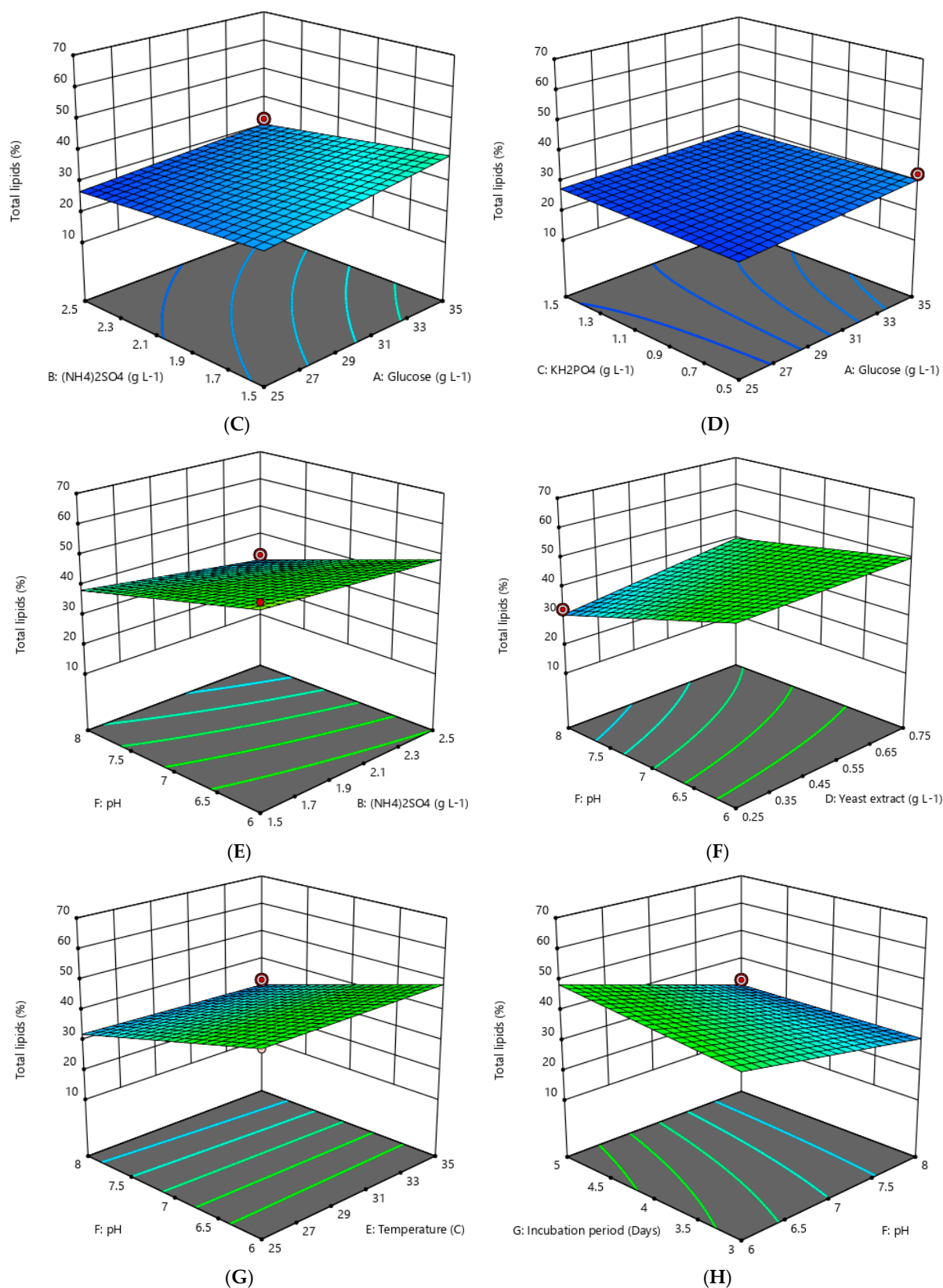


**Figure 3.** Three-dimensional plots of lipid accumulation by oleaginous yeast exhibit the impacts of some combined cultural and environmental parameters: (A) interaction of glucose/pH; (B) interaction of glucose/yeast extract; (C) interaction of glucose/(NH<sub>4</sub>)<sub>2</sub>SO<sub>4</sub>; (D) interaction of glucose/KH<sub>2</sub>PO<sub>4</sub>; (E) interaction of pH/(NH<sub>4</sub>)<sub>2</sub>SO<sub>4</sub>; (F) interaction of yeast extract/pH; (G) interaction of pH/temperature; and (H) interaction of incubation period/pH.

### 3.3. Biodiesel Synthesis from Extracted Lipids of Oleaginous Yeast Biomasses

In the current study, the oleaginous yeast was used as a source for biodiesel synthesis through a chemical transesterification process. The obtained data GC/MS analysis of the produced biodiesel were 82.12% FAMES of the total analytes (Figure 4). The composition analysis of the produced biodiesel revealed that nananedioic (retention time (RT), 27.34), hexadecanoic (RT, 40.5), 9, 12-octadecandienoic (RT, 46.32), 11-octadecenoic (RT, 46.49), octadecanoic (RT, 47.14), and cyclopropanebutanoic (RT, 53.12) methyl esters were the most prevalent methyl esters, comprising 0.5, 30.04, 0.36, 39.36, 6.16, and 0.6% of total esters, respectively (Figure 4). The obtained results revealed the feasibility of oleaginous yeast lipids as a promising feedstock for biodiesel synthesis.

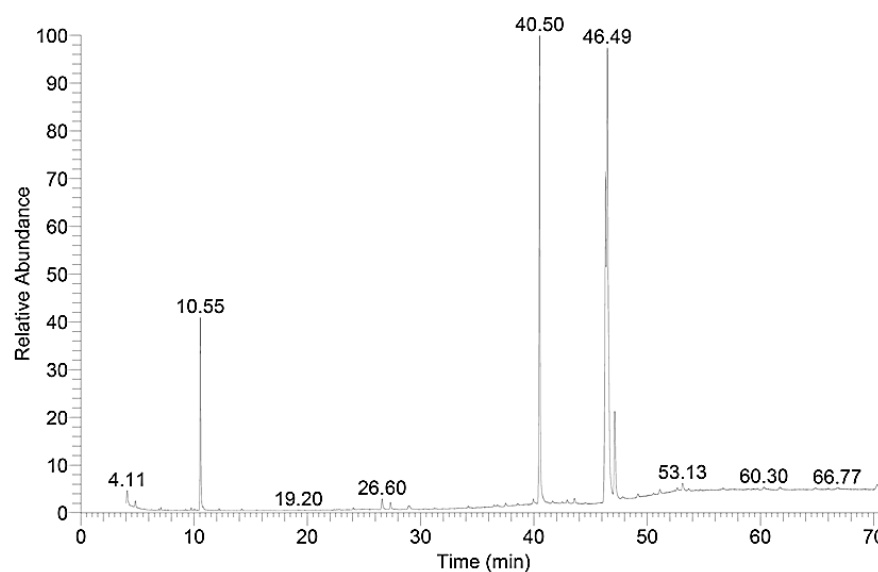


**Figure 4.** GC/MS graph showing the composition of biodiesel produced from the chemical transesterification process of oleaginous yeast lipids.

### 3.4. Quality of the Produced Biodiesel

The quality of biodiesel produced from the transesterification process of yeast lipids were assayed from the calculated physico-chemical characteristics. The obtained results revealed that the biodiesel characteristics, including density ( $0.89 \text{ g cm}^{-3}$ ), kinematic viscosity ( $3.99 \text{ mm}^2 \text{ s}^{-1}$ ), saponification number (151.19), iodine value (34.34), higher heating value ( $42.72 \text{ MJ kg}^{-1}$ ), and Cetane Number (63.86) were fit with the standard US ASTM D6751 and EU EN 14214. In addition, the proportion of FAME with double bonds (C18:2) was 0.36%; FAME with more than four double bonds was not recorded in the produced biodiesel (Table 6).

**Table 6.** The physico-chemical characteristics of fatty acid methyl esters produced by transesterification of yeast lipids.

Character	Value	Standard	
		US Biodiesel Standard ASTM D6751	EU Biodiesel Standard EN 14214
Density ( $\text{g}\cdot\text{cm}^{-3}$ )	0.89	NS	0.86–0.90
Viscosity ( $40 \text{ }^\circ\text{C}$ ; $\text{mm}^2 \text{ s}^{-1}$ )	3.99	1.9–6.0	3.5–5.0
SN	151.19	NS	NS
IV	34.34	NS	120 max
HHV ( $\text{MJ kg}^{-1}$ )	42.72	NS	NS
CN	63.86	47–65	51 min
Concentration of linolenic acid (C18:2) (%)	0.36	NS	12 max
FAME with $\geq 4$ double bonds (%)	ND	NS	1 max

### 3.5. Biosorption of Congo Red

#### 3.5.1. Impact of pH on Removal of Congo Red

The impacts of pH on the biosorption of Congo red from aquatic solution by de-oiled biomass was assayed at an initial Congo red concentration of  $50 \text{ mg L}^{-1}$ , with 15 min contact time, at  $30^\circ\text{C}$ . The obtained data revealed that the decolorization percent of Congo red was enhanced by increasing the pH value of the solution from 2.0 to 6.0, and then the biosorption efficiency decreased (Figure 5).

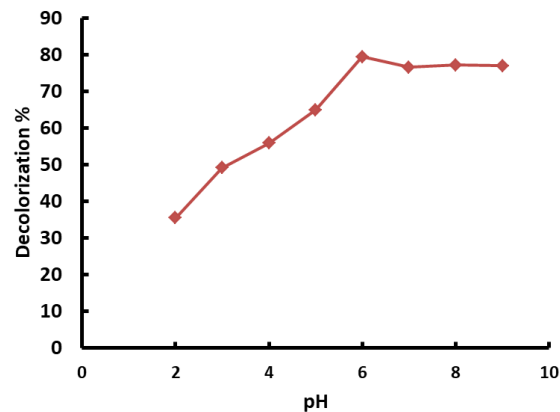


Figure 5. Effect of pH on the removal of Congo red.

#### 3.5.2. Impact of Contact Time

The impact of contact time on Congo red removal by de-oiled yeast biomass was explained in Figure 4. The potential removal of Congo red by the waste biomass took place rapidly within about 15 min, removing 83.9% of the Congo red; then, equilibrium was noticed by increasing time by more than 15 min, and at the short equilibrium time (15 min) as shown in Figure 6.

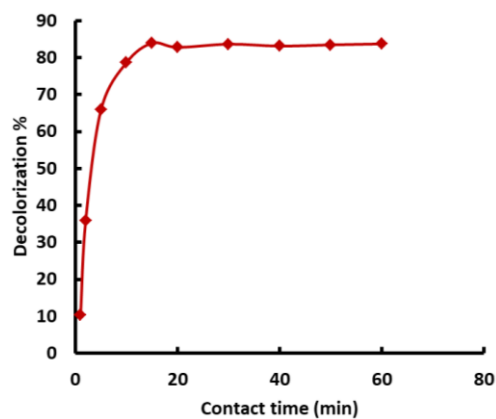


Figure 6. Effect of contact time on the removal of Congo red.

### 3.6. Biosorption Isotherm

Langmuir isotherm was assayed to the biosorption results of Congo red by de-oiled yeast biomasses. The mathematical equation (Equation (10)) used in the Langmuir model was as follows:

$$q_{\text{eq}} = \frac{q_{\text{max}} \times b \times C_{\text{eq}}}{1 + b \times C_{\text{eq}}} \quad (10)$$

and the linear Langmuir formula (Equation (11)) is

$$\frac{C_{\text{eq}}}{q_{\text{eq}}} = \frac{1}{q_{\text{max}} \times b} + \frac{C_{\text{eq}}}{q_{\text{max}}} \quad (11)$$

$C_{eq}$  = the Congo red equilibrium concentration ( $\text{mg L}^{-1}$ ),

$q_{eq}$  = equilibrium adsorption amount ( $\text{mg g}^{-1}$ ).

$q_{max}$  = maximum biosorption capability of the dye per gram of de-oiled biomass ( $\text{mg g}^{-1}$ ).

$b$  = Langmuir constant ( $\text{L mg}^{-1}$ ) represents the de-oiled yeast biomass/Congo red affinity ( $\text{L mg}^{-1}$ ). The values ( $b$ ) and  $q_{max}$  can be determined from the values of the intercept and slope of  $C_{eq}/q_e$  versus the  $C_{eq}$  plot.

The biosorption of Congo red by de-oiled yeast biomasses was applied at initial Congo red concentrations (10–100  $\text{mg L}^{-1}$ ), contact time (15 min), and pH 6 (Figure 7). When the Congo red concentration increased, the biosorption efficiency reduced. Figure 8 shows the relationship between the amount of Congo red dye adsorbed by de-oiled yeast biomasses versus the Congo red dye concentration remaining in the solution and the obtained data were fitted well with the Langmuir model. The calculated Langmuir parameters showed that the highest biosorption capability ( $q_{max}$ ) of Congo red by de-oiled yeast biomasses was  $81.697 \text{ mg g}^{-1}$ , the calculated ( $b$ ) was  $0.24 \text{ L mg}^{-1}$  and correlation coefficients ( $R_2$ ) was 0.977.

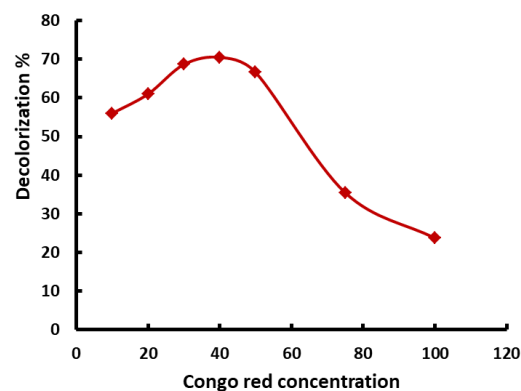


Figure 7. Effect of Congo red concentration ( $\text{mg L}^{-1}$ ) on the removal efficiency.

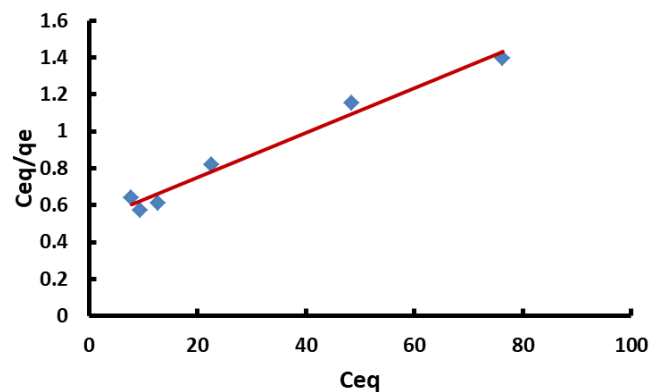


Figure 8. The linear Langmuir formula for adsorption isotherm of Congo red dye by de-oiled yeast biomass wastes.

### 3.7. Fourier-Transform Infrared Spectroscopy (FTIR) Analysis of De-Oiled Biomass Wastes

The obtained results of the FTIR spectra of the functional group for de-oiled biomass revealed the existence of a hydroxyl (OH) group at  $3385.80 \text{ cm}^{-1}$ , amino (NH) group at  $2925.21 \text{ cm}^{-1}$ , methylene ( $\text{CH}_2$ ) groups at  $2854 \text{ cm}^{-1}$ , carbonyl (C=O) group at  $1747 \text{ cm}^{-1}$ , phosphate ( $\text{PO}_4$ ) groups at  $1239 \text{ cm}^{-1}$ , and the shifting of organic phosphate groups ( $\text{PO}_2^{-3}$ ) at  $1078 \text{ cm}^{-1}$  (Figure 9).

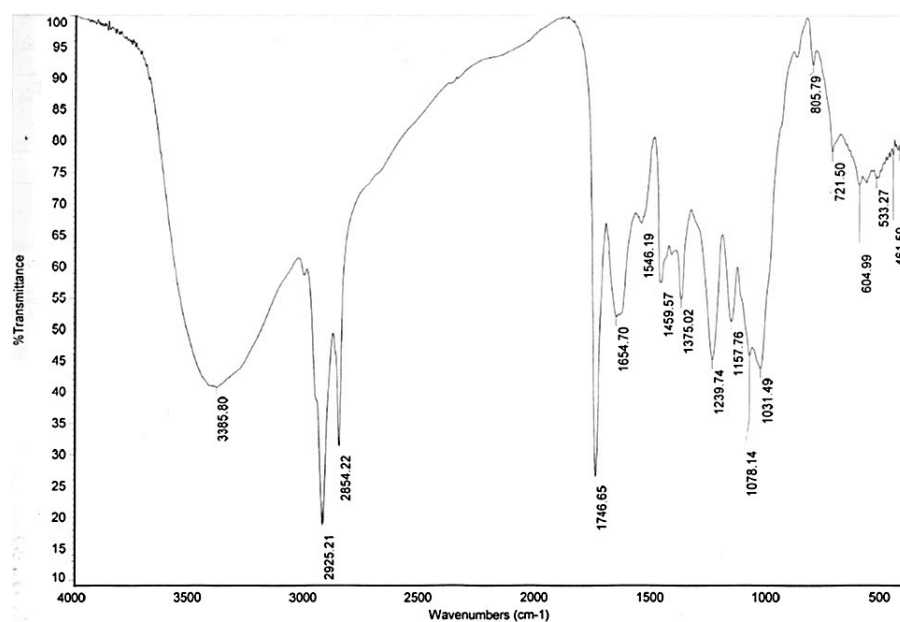


Figure 9. FTIR analysis of de-oiled biomass wastes.

#### 4. Discussion

It was reported that carbohydrates and other substrates can be metabolized into intracellular lipids by a variety of bacteria, algae, yeasts, and fungi. Microbes are classified as “oleaginous” if intracellular lipid accumulation amounts are higher than 20% of the cell dry weight (CDW). Thus, the tested yeast isolate *Rhodotorula toruloides* Y1124 was considered a potent oleaginous microorganism, exhibiting a high lipid content of 47.83% and yeast dry mass of  $7.8 + 1.5 \text{ g L}^{-1}$ . *Rhodotorula toruloides* (formerly known as *Rhodosporidium toruloides*) is red yeast, first isolated from the air in China in 1922 and named *Torula rubescens* [37]. *R. toruloides* is a heterothallic and dimorphism yeast (that exists either in the unicellular yeast morph or as a mycelial morph), and was recorded in different habitats [41,42]. *R. toruloides* is related to the phylum Basidiomycota; class Microbotryomycetes; order Sporidiobolales; and family Sporidiobolaceae [43]. *R. toruloides* showed a high potentiality to accumulate intracellular lipids (single cell oil) to more than 70% of its cell dry weight [44] as well as produce value-added green chemicals, e.g., fatty alcohols, fatty acid esters, carotenoids, sesquiterpenes, and (bio-cement) building block chemicals [45]. Due to the huge demand in the food industry, using lipids produced from edible feedstock for large-scale biodiesel production is not a sustainable practice [46]. Thus, a search for innovative non-edible materials is required to fulfill this requirement. Non-edible feedstocks are considered alternative resources for biodiesel manufacturing that can lower feedstock prices [46]. Oleaginous microorganisms are currently thought to be the most effective feedstock for the manufacture of biodiesel [47] because of their similarity to vegetable oils. Microbial oils have a number of advantages, including productivity that is typically higher than that of plants or vegetable oils, easier upstream and downstream processing, simple genetic modification for high lipid yields, and the ability to grow in a controlled environment independent of the weather or geography [48,49]. In addition to these fascinating features, some oleaginous yeast can use organic wastes as carbon sources for lipid biosynthesis [50], and utilizing different low-cost substrates, like municipal and agricultural organic waste, could indicate a commercially viable synthesis of microbial lipids. This strategy has the combined benefit of lowering the need for waste treatment and disposal while also producing lipids for various industrial uses, which can undoubtedly aid in the shift from a linear to a regenerative circular economy [50]. On the hand, the downstream processes, such as yeast harvesting, cell disruption, lipid extraction, and the high-cost organic substrates, are considered the

important obstacles to be overcome for rendering microbial lipid production economically viable [51,52].

Various yeast species showed intracellular lipid accumulation levels that can exceed 80% of CDW, including *Rhodotorula* sp. (formerly known as *Rhodospiridium*), *Yarrowia lipolytica*, and *Lipomyces* sp. Interestingly, the oleaginous yeast *Rhodospiridium toruloides* was considered an industrial potential single-cell microbe that showed a high potential to accumulate higher amounts of lipids that were used as a feedstock for biodiesel production [53–55]. In the current investigation, we aimed to optimize lipid accumulation by the yeast isolate *Rhodotorula toruloides* Y1124 using the Plackett–Burman design and central composite design in order to maximize the lipid accumulation capability by the oleaginous yeast for biodiesel production. Then, the de-oiled yeast wastes that remained after lipid extraction for biodiesel production were utilized as biosorbents for the removal of toxic Congo red dyes from aquatic solutions. Increasing intracellular lipid accumulation can be accomplished by determining the best conditions for culture and the ideal composition of the medium [56]. In addition, many fermentation factors are suggested to be responsible for the efficient accumulation of lipids. For this purpose, the approaches for designing statistical experiments could offer a scientific and effective way to achieve goals and objectives while also exploring a number of control factors. Consequently, these techniques can be applied to analyze and improve these operational factors, as well as to understand the interaction effects of various parameters [57–59].

#### 4.1. Optimization of Lipid Accumulation by Oleaginous Yeast

In this context, improving the cultivation conditions and nutritional variables is necessary to increase lipid accumulation by oleaginous microorganisms [57]. In addition, the lipid content and profiles of oleaginous microorganisms differ depending on the environment and conditions of cultivation, including the culture medium's composition, nutrients, pH, temperature, and the tested microbe [60]. To increase lipid productivity, the previously mentioned parameters should be optimized because they have a prevalent impact on oleaginous microorganism development and lipid synthesis. The obtained data from the tested design revealed that the tested variables, glucose, temperature and ammonium sulphate, were the most significant factors, whereas the central composite design revealed that the glucose concentration and incubation temperature were the most effective parameters and significantly impacted lipid accumulation yielding the highest lipid content (64.8%). The amount of lipids obtained by oleaginous yeast using the statistical design of optimized variables is quite good compared with previously published data (Table 7). In addition, the optimum culture and environmental parameters for lipid accumulation by *Rhodotorula toruloides* were recorded at glucose concentration ( $38 \text{ g L}^{-1}$ ),  $(\text{NH}_4)_2\text{SO}_4$  ( $2 \text{ g L}^{-1}$ ),  $\text{KH}_2\text{PO}_4$  ( $1 \text{ g L}^{-1}$ ), yeast extract ( $0.5 \text{ g L}^{-1}$ ), initial pH value 7, and an incubation temperature of  $30 \text{ }^\circ\text{C}$  for an incubation period of 4 days.

**Table 7.** Lipid accumulation by various oleaginous yeasts.

Yeast Isolates	Maximum Lipid Content %	References
<i>Yarrowia lipolytica</i>	26.02	[61]
<i>Rhodotorula toruloides</i>	43.80	[62]
<i>Candida tropicalis</i> ASY2	45.96	[63]
<i>Lipomyces starkeyi</i>	28.40	[64]
<i>Cryptococcus curvatus</i> MTCC 2698	28.30	[65]
<i>Trichosporon cutaneum</i>	49.10	[66]
<i>Rhodospiridium toruloides</i> A29	53.51	[67]
<i>Yarrowia lipolytica</i> NCIM 3589	64.50	[68]
<i>Rhodotorula toruloides</i> Y1124	64.80	This study

Interestingly, it was reported that the statistical design analysis for lipid production enhancement by *Rhodotorula* sp. IIP- using response surface methodology revealed that the tested variables pentose sugar, yeast extract,  $\text{KH}_2\text{PO}_4$ ,  $(\text{NH}_4)_2\text{SO}_4$ , temperature, and pH significantly affect lipid production [69]. In addition, the results of Plackett–Burman statistical design for the enhancement of lipid production by *Pichia cactophila* stated that the most effective parameters were glycerol, yeast extract, urea, and  $\text{NH}_4\text{NO}_3$  [70]. Furthermore, Thangavelu et al. [63] reported that under the optimum conditions for lipid production by *Candida tropicalis* ASY2, the highest yield ( $2.68 \text{ g L}^{-1}$ ) was recorded with starch content,  $15.33 \text{ g L}^{-1}$ ; yeast extract,  $0.5 \text{ g L}^{-1}$ ; and airflow rate in a bioreactor  $5.992 \text{ L min}^{-1}$ . Saran et al. [67] stated that the highest lipid accumulation by *R. toruloides* was attained using RSM optimized medium containing  $75 \text{ g L}^{-1}$  glucose;  $2.75 \text{ g L}^{-1}$   $\text{NaNO}_3$ ;  $2.5 \text{ g L}^{-1}$  yeast extract; and  $0.5 \text{ g L}^{-1}$   $\text{MgSO}_4$ , and the production was scaled up in a 30 L bioreactor, resulting in a 22-fold increase in lipid content. Interestingly, Li et al. [71] stated that the majority of lipid-producing microorganisms were known to utilize glucose to accumulate higher levels of lipids. In addition, the highest lipids contents (52.42%) were recorded in the presence of yeast extract as nitrogen sources, while inorganic nitrogen sources were better for microbial cell growth than lipid accumulation [72]. According to several studies, the carbon concentration of the culture medium was found to have a significant impact on microbial lipid synthesis by oleaginous yeasts [73,74]. Furthermore, Karim et al., [58] reported that lipid synthesis increases with longer incubation times in the early stages of operation, but it starts to decline after a few days of operation due to the microbial breakdown of stored lipids. This suggests that incubation time has a significant impact on the performance of lipid accumulation. It is widely known that oleaginous microorganisms first store lipids, particularly during the lag/log phase, and begin to degrade lipids under carbon-deficient conditions [75].

Consequently, yeasts are distinguished by their rapid developments, short life cycles, lack of dependence on light energy, simple to scale-up, and utilization of a variety of carbon sources [18]. Consequently, a substantial number of studies was carried out to improve microbial oil production by oleaginous fungi [76–81]. Oleaginous yeasts are considered potential alternatives to petro-oil and available oil resources for biodiesel production [82]. In this study, the chemical transesterification process of *Rhodotorula toruloides* lipids recorded biodiesel yield 82.12% FAMES of the total analytes and the most common fatty acid methyl esters were hexadecanoic methyl ester (C17:0) and 11-octadecenoic methyl ester (C19:1) comprising 30.04 and 39.36% of total methyl esters, respectively. In addition, nananedioic, octadecanoic, and cyclopropanebutanoic methyl esters were also detected, which revealed the compatibility of oleaginous yeast lipids with plant oils [70]. Furthermore, the obtained results of the biodiesel quality characteristics in the current study were compatible with the range of the standard characteristics of US ASTM D6751 biodiesel and EU EN 14214. Thus, the obtained results revealed the feasibility of oleaginous yeast lipids as a promising feedstock for biodiesel synthesis. Due to the variable fatty acid content of biodiesel, it has various physicochemical characteristics. The main factors that determine the qualities of biodiesel are its composition of fatty acids, including saturated, monounsaturated, and polyunsaturated fatty acids. Three criteria, namely oxidation, thermal, and storage stabilities, can be used to analyze biodiesel stability. The most crucial of these criteria is oxidation stability due to biodiesel having a low oxidation tolerance. Oxidation stability is significantly related to the degree of unsaturation and the number of double bonds in the polyunsaturated fatty acid chain in the ester molecule, which readily react with air to degrade biodiesel oxidation stability. In addition, other crucial biodiesel characteristics and quality like density, kinematic viscosity, cetane number, acid value, pour and cold filter plugging points may also degrade further [19,83].

#### 4.2. Biosorption of Congo Red by De-Oiled Yeast Biomasses

The impacts of pH on the biosorption of Congo red by de-oiled biomass showed that the Congo red decolorization percent was enhanced by increasing the pH value of the solution until pH value was 6.0, at which point the decolorization efficiency decreased. In acidic solutions, hydrogen proton ( $H^+$ ) is easily joined with  $SO_3^-$  groups in Congo red, so the decolorization percent increased through the electrostatic attraction force between molecules [84], whereas in the alkaline solution ( $pH > 7$ ),  $OH^-$  groups increased in the solution, and at the same time the yeast cell walls contained many negative charges; consequently, there was an electrostatic repulsion force between de-oiled yeast biomasses and Congo red dye [85], resulting in a decrease in the Congo red decolorization rate.

The results of Congo red removal by increasing contact time revealed the potential of de-oiled yeast biomasses for removing Congo red from contaminated wastewater within 15 min, removing 83.9%, and this may be due to available binding sites for Congo red particles on the de-oiled yeast biosorbents. The obtained results indicated that the Congo red can be absorbed freely by the de-oiled yeast active sites, so the adsorbed amount increases rapidly; then, the active sites are filled by the Congo red dye and the adsorption capability decreases [86].

Biosorption isotherm using the Langmuir model was assessed for the Congo red biosorption data using de-oiled yeast biomasses [87,88]. The obtained data revealed that, when the Congo red concentration increased in solution, the removal efficiency decreased due to the saturation of the adsorption active sites on the adsorbent [89]. In addition, the obtained data illustrating the relationship between the Congo red amount adsorbed and the residual Congo red concentration in the solution fitted well with the Langmuir model. Furthermore, the calculated Langmuir parameters revealed that the  $q_{max}$  was  $81.70 \text{ mg g}^{-1}$  and the calculated (b) was  $0.24 \text{ L mg}^{-1}$ , indicating the de-oiled yeast biomass-biosorbent affinities, and this shows that Congo red was favorably adsorbed by the de-oiled yeast biomasses [90]. The high correlation coefficients ( $R_2 = 0.977$ ) indicated that the Langmuir model explains the Congo red biosorption equilibrium by the de-oiled biomass in the tested concentration ranges. It was stated that the Langmuir isotherm depends on the hypothesis of monolayer coverage of the tested dye onto a biosorbent with the homogenous surface, i.e., the biosorbent consists of similar sites with equal binding energy [91].

The biomass of microorganisms showed many functional groups that had the potential to sequester toxic dyes in aquatic solutions [21,92]. The FTIR spectra of de-oiled biomass revealed the existence of many functional groups such as hydroxyl (OH), amino (NH), methylene ( $CH_2$ ), carbonyl (C=O), and phosphate ( $PO_4$ ) groups. The presence of these characteristic functional groups could explain the mechanism of the biosorption process. The biosorption mechanism may be illustrated through the electrostatic interaction by opposite charges of the biosorbent and Congo red. The presence of the positively charged  $NH_4^+$  of Congo red encourages the electrostatic force with negatively charged  $PO_4^{3-}$  and  $COO^-$ . In addition, the negatively charged sulfonate groups of CR may be electrostatically attracted to the amine groups of the adsorbent. Because of the recording of H-donor groups like  $OH^-$ ,  $COO^-$ ,  $NH_2$ , and  $CH_2$  on the adsorbent surface, a hydrogen-bonding interaction with Congo red will take place during the adsorption process. Furthermore, the Biosorption mechanism may be due to the formation of H bonds between the nitrogen or sulfur atoms of the Congo red dye and OH and COOH groups [93], or due to Yoshida-bonding occurring between the aromatic rings of CR and H-donor groups of the de-oiled yeast biomass [94]. Similarly, it was implied that the  $CH_2$  and  $CH_3$  groups were involved in the H-bonding [95,96].

#### 5. Conclusions

The obtained results for optimizing the lipid accumulation process by the biomass of *Rhodotorula toruloides* revealed that the optimum conditions were glucose concentration ( $38 \text{ g L}^{-1}$ ),  $(NH_4)_2SO_4$  ( $2 \text{ g L}^{-1}$ ),  $KH_2PO_4$  ( $1 \text{ g L}^{-1}$ ), yeast extract ( $0.5 \text{ g L}^{-1}$ ), temperature  $30^\circ\text{C}$ , pH 7, and an incubation period of 4 days, which resulted in 64.8% of the total lipids

being accumulated. The produced biodiesel yield from yeast biomass was 82.12% FAMES and the most dominant fatty acid methyl ester was 11-octadecenoic, which accounted for 39.36% of total methyl esters. Biodiesel production from low-cost oleaginous yeast showed a potential applicability, but the extraction technique of microbial lipid is considered a major limitation. In the current study, the de-oiled biomass wastes were reutilized after biodiesel synthesis as a biosorbent and showed a high efficiency in removing Congo red dyes from aquatic solutions. The maximal biosorption capacity ( $q_{max}$ ) was  $81.697 \text{ mg g}^{-1}$ , and this may attributed to the unique structures of functional groups of the de-oiled biomass, such as COOH, OH,  $\text{NH}_2$ , and  $\text{CH}_2$  that facilitate the biosorption process through electrostatic forces, hydrogen bonding, and ion exchange mechanisms. The limitation of this technique in the downstream process includes the separation and collection of the biosorbent after the biosorption process, and this drawback may be compensated for by using a low-cost biological immobilizing agent. The present study revealed that oleaginous yeast lipids may provide a prospective low-cost, eco-friendly feedstock for biodiesel synthesis, as well as having the potential to be applied in de-oiled biomass wastes for Congo red dye removal.

**Supplementary Materials:** The following supporting information can be downloaded at: <https://www.mdpi.com/article/10.3390/su151813412/s1>, Table S1: The quadratic model of the experimental design assayed for study the effect of the nutritional and environmental conditions on lipid accumulation by the oleaginous yeast using Plackett–Burman design; Table S2: The experimental design assayed for study the effect of the nutritional and environmental conditions on lipid accumulation by the oleaginous yeast using central composite design.

**Author Contributions:** E.A.H., S.H. and A.N.: designed the experimental work; methodology; software, formal analysis; data curation; writing—original draft preparation; and writing—review and editing; M.S.A., S.A., N.Z., E.I.A., A.N., K.A., T.S.A. and T.A.: supervision; formal analysis; investigation; data curation; and writing—review and editing; M.S.A.: revision the manuscript; visualization; project administration; and funding acquisition. All authors have read and agreed to the published version of the manuscript.

**Funding:** This project was funded by the Deanship of Scientific Research (DSR) at King Abdulaziz University, Jeddah, under grant no. G: 441-140-1442.

**Institutional Review Board Statement:** Not applicable

**Informed Consent Statement:** Not applicable

**Data Availability Statement:** Not applicable.

**Acknowledgments:** The authors gratefully acknowledge the DSR's technical and financial support.

**Conflicts of Interest:** The authors declare no conflict of interest.

## Abbreviations

ANOVA	Analysis of variance
$\text{CaCl}_2 \cdot 2\text{H}_2\text{O}$	Calcium chloride dihydrate
CCD	Central composite design
CR	Congo red
FAMES	fatty acid methyl esters
FTIR	Fourier-transform infrared spectroscopy
GC/MS	Gas chromatography/mass spectrum
KBr	Potassium bromide
$\text{KH}_2\text{PO}_4$	Potassium dihydrogen phosphate
$\text{MgSO}_4 \cdot 7\text{H}_2\text{O}$	Magnesium sulfate heptahydrate
NaCl	Sodium chloride
$(\text{NH}_4)_2\text{SO}_4$	Ammonium sulfate
PBD	Plackett–Burman design
YMA	Yeast malt extract agar medium

## References

1. Holechek, J.L.; Geli, H.M.; Sawalhah, M.N.; Valdez, R. A global assessment: Can renewable energy replace fossil fuels by 2050? *Sustainability* **2022**, *14*, 4792. [[CrossRef](#)]
2. Chuba, V.; Lavrinenko, A.; Chuba, V.; Tsyvenkova, N. Justification of fuel mixture composition of petroleum based diesel fuel and diesel biofuel based on plant oil. In *Engineering for Rural Development. Proceedings of the International Scientific Conference (Latvia)*; Latvia University of Life Sciences and Technologies: Jelgava, Latvia, 2021. [[CrossRef](#)]
3. Abd-Alla, M.H.; Bagy, M.M.K.; Morsy, F.M.; Hassan, E.A. Enhancement of biodiesel, hydrogen and methane generation from molasses by *Cunninghamella echinulata* and anaerobic bacteria through sequential three-stage fermentation. *Energy* **2014**, *78*, 543–554. [[CrossRef](#)]
4. Najjar, A.A.; Hassan, E.A.; Zabermaawi, N.M.; Almasaudi, S.B.; Moulay, M.; Harakeh, S.; Abd El-Aal, M. Efficacy of the Immobilized *Kocuria flava* Lipase on Fe<sub>3</sub>O<sub>4</sub>/Cellulose Nanocomposite for Biodiesel Production from Cooking Oil Wastes. *Catalysts* **2022**, *12*, 977. [[CrossRef](#)]
5. El-Sheekh, M.M.; Ibrahim, H.A.; Barakat, K.M.; Shaltout, N.A.; Sayed, W.M.E.; Abou-Shanab, R.A.; Sadowsky, M.J. Potential of Marine Biota and Bio-waste Materials as Feedstock for Biofuel Production. In *Waste Management*; CRC Press: Boca Raton, FL, USA, 2022; pp. 123–139.
6. Bagy, M.M.K.; Abd-Alla, M.H.; Morsy, F.M.; Hassan, E.A. Two stage biodiesel and hydrogen production from molasses by oleaginous fungi and *Clostridium acetobutylicum* ATCC 824. *Int. J. Hydrogen Energy* **2014**, *39*, 3185–3197. [[CrossRef](#)]
7. Yaashikaa, P.R.; Kumar, P.S.; Karishma, S. Bio-derived catalysts for production of biodiesel: A review on feedstock, oil extraction methodologies, reactors and lifecycle assessment of biodiesel. *Fuel* **2022**, *316*, 123379. [[CrossRef](#)]
8. Abd-Alla, M.H.; Bagy, M.M.K.; Morsy, F.M.; Hassan, E.A. Improvement of fungal lipids esterification process by bacterial lipase for biodiesel synthesis. *Fuel* **2015**, *160*, 196–204. [[CrossRef](#)]
9. Kumbhar, M.B.; Lokhande, P.E.; Chavan, U.S.; Salunkhe, V.G.A. Global Scenario of Sustainable Technologies and Progress in a Biodiesel Production. In *Biodiesel Technology and Applications*; Inamuddin Ahamed, M.I., Boddula, R., Rezakazemi, M., Eds.; John Wiley & Sons, Inc.: Hoboken, NJ, USA, 2021; pp. 215–240. [[CrossRef](#)]
10. Azizian, H.; Kramer, J.K. A rapid method for the quantification of fatty acids in fats and oils with emphasis on trans fatty acids using Fourier transform near infrared spectroscopy (FT-NIR). *Lipid* **2005**, *40*, 855–867. [[CrossRef](#)]
11. Balat, M. Potential alternatives to edible oils for biodiesel production—A review of current work. *Energy Convers. Manag.* **2011**, *52*, 1479–1492. [[CrossRef](#)]
12. Gui, M.M.; Lee, K.; Bhatia, S. Feasibility of edible oil vs. non-edible oil vs. waste edible oil as biodiesel feedstock. *Energy* **2008**, *33*, 1646–1653. [[CrossRef](#)]
13. Rincón, L.; Jaramillo, J.; Cardona, C. Comparison of feedstocks and technologies for biodiesel production: An environmental and technoeconomic evaluation. *Ren. Energy* **2014**, *69*, 479–487. [[CrossRef](#)]
14. Nguyen, H.C.; Liang, S.H.; Chen, S.S.; Su, C.H.; Lin, J.H.; Chien, C.C. Enzymatic production of biodiesel from insect fat using methyl acetate as an acyl acceptor: Optimization by using response surface methodology. *Energy Conv. Manag.* **2018**, *158*, 168–175. [[CrossRef](#)]
15. Nguyen, H.C.; Nguyen, M.L.; Wang, F.M.; Juan, H.Y.; Su, C.H. Biodiesel production by direct transesterification of wet spent coffee grounds using switchable solvent as a catalyst and solvent. *Biores. Technol.* **2020**, *296*, 122334. [[CrossRef](#)] [[PubMed](#)]
16. Awais, M.; Musmar, S.E.A.; Kabir, F.; Batool, I.; Rasheed, M.A.; Jamil, F.; Khan, S.U.; Tlili, I. Biodiesel production from *Melia azedarach* and *Ricinus communis* oil by transesterification process. *Catalysts* **2020**, *10*, 427. [[CrossRef](#)]
17. Chopra, J.; Rangarajan, V.; Sen, R. Recent developments in oleaginous yeast feedstock based biorefinery for production and life cycle assessment of biofuels and value-added products. *Sustain. Energy Technol. Assess.* **2022**, *53*, 102621. [[CrossRef](#)]
18. Bao, W.; Li, Z.; Wang, X.; Gao, R.; Zhou, X.; Cheng, S.; Men, Y.; Zheng, L. Approaches to improve the lipid synthesis of oleaginous yeast *Yarrowia lipolytica*: A review. *Ren. Sustain. Energy Rev.* **2021**, *149*, 111386. [[CrossRef](#)]
19. Uğuz, G.; Atabani, A.E.; Mohammed, M.N.; Shobana, S.; Uğuz, S.; Kumar, G.; Ala'a, H. Fuel stability of biodiesel from waste cooking oil: A comparative evaluation with various antioxidants using FT-IR and DSC techniques. *Biocat. Agric. Biotechnol.* **2019**, *21*, 101283. [[CrossRef](#)]
20. Beopoulos, A.; Cescut, J.; Haddouche, R.; Uribebarrea, J.L.; Molina-Jouve, C.; Nicaud, J.M. *Yarrowia lipolytica* as a model for bio-oil production. *Prog Lipid Res.* **2009**, *48*, 375–387. [[CrossRef](#)]
21. Grossart, H.P.; Hassan, E.A.; Masigol, H.; Arias-Andres, M.; Rojas-Jimenez, K. Inland Water Fungi in the Anthropocene: Current and Future Perspectives. In *The Encyclopedia of Inland Waters*, 2nd ed.; Kendra Cheruvilil; Elsevier: Amsterdam, The Netherlands, 2021.
22. Llorca, M.; Farré, M.; Eljarrat, E.; Díaz-Cruz, S.; Rodríguez-Mozaz, S.; Wunderlin, D.; Barcelo, D. Review of emerging contaminants in aquatic biota from Latin America: 2002–2016. *Environ. Toxicol. Chem.* **2017**, *36*, 1716–1727. [[CrossRef](#)]
23. Rodríguez-Castillo, G.; Molina-Rodríguez, M.; Cambronero-Heinrichs, J.C.; Quirós-Fournier, J.P.; Lizano-Fallas, V.; Jiménez-Rojas, C.; Masis-Mora, M.; Castro-Gutiérrez, V.; Mata-Araya, I.; Rodríguez-Rodríguez, C.E. Simultaneous removal of neonicotinoid insecticides by a microbial degrading consortium: Detoxification at reactor scale. *Chemosphere* **2019**, *235*, 1097–1106. [[CrossRef](#)]

24. Official Journal of the European Union. Commission Implementing Decision (EU) 2015/495 of 20 March 2015 Establishing a Watch List of Substances for Union-Wide Monitoring in the Field of Water Policy Pursuant to Directive 2008/105/EC of the European Parliament and of the Council (Notified under Document C(2015) 1756) Text with EEA Relevance. 2015. Available online: <https://leap.unep.org/countries/eu/national-legislation/commission-implementing-decision-eu-2015495-establishing-watch> (accessed on 4 June 2023).
25. Sun, B.; Li, Q.; Zheng, M.; Su, G.; Lin, S.; Wu, M.; Li, C.; Wang, Q.; Tao, Y.; Dai, L.; et al. Recent advances in the removal of persistent organic pollutants (POPs) using multifunctional materials: A review. *Environ. Poll.* **2020**, *265*, 114908. [\[CrossRef\]](#)
26. Rath, B.S.; Kumar, P.S.; Vo, D.V.N. Critical review on hazardous pollutants in water environment: Occurrence, monitoring, fate, removal technologies and risk assessment. *Sci. Total Environ.* **2021**, *797*, 149134. [\[CrossRef\]](#) [\[PubMed\]](#)
27. Nozaki, K.; Beh, C.H.; Mizuno, M.; Isobe, T.; Shiroishi, M.; Kanda, T.; Amano, Y. Screening and investigation of dye decolorization activities of basidiomycetes. *J. Biosci. Bioeng.* **2008**, *105*, 69–72. [\[CrossRef\]](#)
28. Greluk, M.; Hubicki, Z. Efficient removal of Acid Orange 7 dye from water using the strongly basic anion exchange resin Amberlite IRA-95. *Desalination* **2011**, *278*, 219. [\[CrossRef\]](#)
29. Tišma, M.; Zelić, B.; Vasić-Rački, Đ. White-rot fungi in phenols, dyes and other xenobiotics treatment—A brief review. *Croatian J. Food Sci. Technol.* **2010**, *2*, 34–47.
30. Kurade, M.B.; Waghmode, T.R.; Jadhav, M.U.; Jeon, B.H.; Govindwar, S.P. Bacterial–yeast consortium as an effective biocatalyst for biodegradation of sulfonated azo dye Reactive Red 198. *RSC Adv.* **2015**, *5*, 23046–23056. [\[CrossRef\]](#)
31. Chung, K.T.; Chen, S.C.; Wong, T.Y.; Li, Y.S.; Wei, C.L.; Chou, M.-W. Mutagenic studies of benxidine and its analogues: Structure activity relationships. *Toxicol. Sci.* **2000**, *56*, 351–356. [\[CrossRef\]](#)
32. Bentahar, S.; Dbik, A.; El Khomri, M.; El Messaoudi, N.; Lacherai, A. Adsorption of methylene blue, crystal violet and congo red from binary and ternary systems with natural clay: Kinetic, isotherm, and thermodynamic. *J. Environ. Chem. Eng.* **2017**, *5*, 5921–5932. [\[CrossRef\]](#)
33. Adeyi, A.A.; Jamil, S.N.; Abdullah, L.C.; Choong, T.S.; Lau, K.L.; Abdullah, M. Simultaneous adsorption of cationic dyes from binary solutions by thiourea-modified poly(acrylonitrile-co-acrylic acid): Detailed isotherm and kinetic studies. *Materials* **2019**, *12*, 2903. [\[CrossRef\]](#)
34. Yang, L.; Zhang, Y.; Liu, X.; Jiang, X.; Zhang, Z.; Zhang, T.; Zhang, L. The investigation of synergistic and competitive interaction between dye Congo red and methyl blue on magnetic MnFe<sub>2</sub>O<sub>4</sub>. *Chem. Eng. J.* **2014**, *246*, 88–96. [\[CrossRef\]](#)
35. Folch, J.; Ascoli, I.; Lees, M.; Meath, J.A.; LeBaron, F.N. Preparation of lipide extracts from brain tissue. *J. Biol. Chem.* **1951**, *191*, 833–841. [\[CrossRef\]](#)
36. Anschau, A.; Caruso, C.S.; Kuhn, R.C.; Franco, T.T. Validation of the sulfo-phospho-vanillin (SPV) method for the determination of lipid content in oleaginous microorganisms". *Braz. J. Chem. Eng.* **2017**, *34*, 19–27. [\[CrossRef\]](#)
37. Banno, I. Studies on the sexuality of *Rhodotorula*. *J. General Appl. Microbiol.* **1967**, *13*, 167–196. [\[CrossRef\]](#)
38. Sampaio, J.P. *Rhodospiridium banno* (1967). In *The Yeasts*; Elsevier: Amsterdam, The Netherlands, 2011; pp. 1523–1539.
39. Vicente, G.; Bautista, L.F.; Gutiérrez, F.J.; Rodríguez, R.; Martínez, V.; Rodríguez-Frómata, R.A.; Ruiz-Vázquez, R.M.; Torres-Martínez, S.; Garre, V. Direct transformation of fungal biomass from submerged cultures into biodiesel. *Energy Fuels* **2010**, *24*, 3173–3178. [\[CrossRef\]](#)
40. Najjar, A.; Hassan, E.A.; Zabermaawi, N.; Saber, S.H.; Bajrai, L.H.; Almuhayawi, M.S.; Abujamel, T.S.; Almasaudi, S.B.; Azhar, L.E.; Moulay, M.; et al. Optimizing the catalytic activities of methanol and thermotolerant *Kocuria flava* lipases for biodiesel production from cooking oil wastes. *Sci. Rep.* **2021**, *11*, 13659. [\[CrossRef\]](#)
41. Singh, G.; Sinha, S.; Kumar, K.K.; Gaur, N.A.; Bandyopadhyay, K.K.; Paul, D. High density cultivation of oleaginous yeast isolates in 'mandi' waste for enhanced lipid production using sugarcane molasses as feed. *Fuel* **2020**, *276*, 118073. [\[CrossRef\]](#)
42. Xue, S.J.; Li, X.C.; Huang, X.; Liu, J.; Li, Y.; Zhang, X.T.; Zhang, J.Y. Diversity investigation of cultivable yeasts associated with honeycombs and identification of a novel *Rhodotorula toruloides* strain with the robust concomitant production of lipid and carotenoid. *Bioresour. Technol.* **2023**, *370*, 128573. [\[CrossRef\]](#) [\[PubMed\]](#)
43. Wen, Z.; Zhang, S.; Odoh, C.K.; Jin, M.; Zhao, Z.K. *Rhodospiridium toruloides*—A potential red yeast chassis for lipids and beyond. *FEMS Yeast Res.* **2020**, *20*, foaa038. [\[CrossRef\]](#)
44. Sajish, S.; Singh, S.; Nain, L. Yeasts for Single Cell Oil Production from Non-conventional Bioresources. In *Microbial Biotechnology for Renewable and Sustainable Energy*; Springer Nature: Singapore, 2022; pp. 337–364.
45. Zhao, Y.; Song, B.; Li, J.; Zhang, J. *Rhodotorula toruloides*: An ideal microbial cell factory to produce oleochemicals, carotenoids, and other products. *World J. Microbiol. Biotechnol.* **2022**, *38*, 13. [\[CrossRef\]](#)
46. Patel, A.; Sartaj, K.; Pruthi, P.A.; Pruthi, V.; Matsakas, L. Utilization of Clarified Butter Sediment Waste as a Feedstock for Cost-Effective Production of Biodiesel. *Foods* **2019**, *8*, 234. [\[CrossRef\]](#)
47. Papanikolaou, S. Oleaginous Yeasts: Biochemical Events Related with Lipid Synthesis and Potential Biotechnological Applications. *Ferment. Technol.* **2012**, *1*, 1000–1103. [\[CrossRef\]](#)
48. Dourou, M.; Aggeli, D.; Papanikolaou, S.; Aggelis, G. Critical steps in carbon metabolism affecting lipid accumulation and their regulation in oleaginous microorganisms. *Appl. Microbiol. Biotechnol.* **2018**, *102*, 2509–2523. [\[CrossRef\]](#)
49. Patel, A.; Karageorgou, D.; Rova, E.; Katapodis, P.; Rova, U.; Christakopoulos, P.; Matsakas, L. An overview of potential oleaginous microorganisms and their role in biodiesel and omega-3 fatty acid-based industries. *Microorganism* **2020**, *8*, 434. [\[CrossRef\]](#) [\[PubMed\]](#)

50. Cho, H.U.; Park, J.M. Biodiesel production by various oleaginous microorganisms from organic wastes. *Bioresour. Technol.* **2018**, *256*, 502–508. [[CrossRef](#)] [[PubMed](#)]
51. Yellapu, S.K.; Bharti Kaur, R.; Kumar, L.R.; Tiwari, B.; Zhang, X.; Tyagi, R.D. Recent developments of downstream processing for microbial lipids and conversion to biodiesel. *Bioresour. Technol.* **2018**, *256*, 515–528. [[CrossRef](#)] [[PubMed](#)]
52. Tomás-Pejó, E.; Morales-Palomo, S.; González-Fernández, C. Microbial lipids from organic wastes: Outlook and challenges. *Bioresour. Technol.* **2021**, *323*, 124612. [[CrossRef](#)]
53. Guo, M.; Cheng, S.; Chen, G.; Chen, J. Improvement of lipid production in oleaginous yeast *Rhodospiridium toruloides* by ultraviolet mutagenesis. *Eng. Life Sci.* **2019**, *19*, 548–556. [[CrossRef](#)] [[PubMed](#)]
54. Alankar, S.S.L.; Sajesh, N.; Rastogi, S.; Sakhuja, S.; Rajeswari, G.; Kumar, V.; Chandel, A.K.; Jacob, S. Bioprocessing of fermentable sugars derived from water hyacinth into microbial lipids and single cell proteins by oleaginous yeast *Rhodospiridium toruloides* NCIM 3547. *Biomass Convers. Biorefinery* **2021**, 1–15. [[CrossRef](#)]
55. Osman, M.E.; Abdel-Razik, A.B.; Zaki, K.I.; Mamdouh, N.; El-Sayed, H. Isolation, molecular identification of lipid-producing *Rhodotorula diobovata*: Optimization of lipid accumulation for biodiesel production. *J. Genet. Eng. Biotechnol.* **2022**, *20*, 32. [[CrossRef](#)]
56. Zhao, X.; Kong, X.; Hua, Y.; Feng, B.; Zhao, Z.K. Medium optimization for lipid production through co-fermentation of glucose and xylose by the oleaginous yeast *Lipomyces starkeyi*. *Eur. J. Lipid Sci. Technol.* **2008**, *110*, 405–412. [[CrossRef](#)]
57. Awad, D.; Bohnen, F.; Mehlmer, N.; Brueck, T. Multi-factorial-guided media optimization for enhanced biomass and lipid formation by the oleaginous yeast *Cutaneotrichosporon oleaginosus*. *Front. Bioeng. Biotechnol.* **2019**, *7*, 54. [[CrossRef](#)]
58. Karim, A.; Islam, M.A.; Mishra, P.; Muzahid, A.J.M.; Yousuf, A.; Khan, M.; Faizal, C.K.M. Yeast and bacteria co-culture-based lipid production through bioremediation of palm oil mill effluent: A statistical optimization. *Biomass Convers. Biorefinery* **2021**, *13*, 2947–2958. [[CrossRef](#)]
59. Baş, D.; Boyacı, I.H. Modeling and optimization I: Usability of response surface methodology. *J. Food Eng.* **2007**, *78*, 836–845. [[CrossRef](#)]
60. Subramaniam, R.; Dufreche, S.; Zappi, M.; Bajpai, R. Microbial lipids from renewable resources: Production and characterization. *J. Ind. Microb. Biotechnol.* **2010**, *37*, 1271–1287. [[CrossRef](#)] [[PubMed](#)]
61. Gao, R.; Li, Z.; Zhou, X.; Bao, W.; Cheng, S.; Zheng, L. Enhanced lipid production by *Yarrowia lipolytica* cultured with synthetic and waste-derived high-content volatile fatty acids under alkaline conditions. *Biotechnol. Biofuel* **2020**, *13*, 3. [[CrossRef](#)] [[PubMed](#)]
62. Lopes, H.J.S.; Bonturi, N.; Kerkhoven, E.J.; Miranda, E.A.; Lahtvee, P.J. C/N ratio and carbon source-dependent lipid production profiling in *Rhodotorula toruloides*. *Appl. Microbiol. Biotechnol.* **2020**, *104*, 2639–2649. [[CrossRef](#)] [[PubMed](#)]
63. Thangavelu, K.; Sundararaju, P.; Srinivasan, N.; Uthandi, S. Bioconversion of sago processing wastewater into biodiesel: Optimization of lipid production by an oleaginous yeast, *Candida tropicalis* ASY2 and its transesterification process using response surface methodology. *Microb. Cell Factories* **2021**, *20*, 167. [[CrossRef](#)]
64. Xavier, M.C.A.; Coradini, A.L.V.; Deckmann, A.C.; Franco, T.T. Lipid production from hemicellulose hydrolysate and acetic acid by *Lipomyces starkeyi* and the ability of yeast to metabolize inhibitors. *Biochem. Eng. J.* **2017**, *118*, 11–19. [[CrossRef](#)]
65. Chatterjee, S.; Mohan, S.V. Microbial lipid production by *Cryptococcus curvatus* from vegetable waste hydrolysate. *Bioresour. Technol.* **2018**, *254*, 284–289. [[CrossRef](#)]
66. Liu, J.; Zhou, W.; He, Q.; Zhao, M.; Gong, Z. Microbial Lipid Production from High Concentration of Volatile Fatty Acids via *Trichosporon cutaneum* for Biodiesel Preparation. *Appl. Biochem. Biotechnol.* **2022**, *194*, 2968–2979. [[CrossRef](#)]
67. Saran, S.; Mathur, A.; Dalal, J.; Saxena, R.K. Process optimization for cultivation and oil accumulation in an oleaginous yeast *Rhodospiridium toruloides* A29. *Fuel* **2017**, *188*, 324–331. [[CrossRef](#)]
68. Raut, G.; Jagtap, S.; Kumar, V.R.; RaviKumar, A. Enhancing lipid content of oleaginous *Yarrowia lipolytica* biomass grown on waste cooking oil and its conversion to biodiesel by statistical optimization. *Biomass Convers. Biorefinery* **2022**, 1–18. [[CrossRef](#)]
69. Bandhu, S.; Dasgupta, D.; Akhter, J.; Kanaujia, P.; Suman, S.K.; Agrawal, D.; Kaul, S.; Adhikari, D.K.; Ghosh, D. *Statistical Design and Optimization of Single Cell Oil Production from Sugarcane Bagasse Hydrolysate by an Oleaginous Yeast Rhodotorula sp. IIP-33 Using Response Surface Methodology*; SpringerPlus, Springer Science and Business Media Deutschland GmbH: Berlin, Germany, 2014; Volume 3, pp. 1–11.
70. Berikten, D.; Hosgun, E.Z.; Bozan, B.; Kivanc, M. Improving lipid production capacity of new natural oleaginous yeast: *Pichia cactophila* firstly. *Biomass Convers. Biorefinery* **2021**, *12*, 1311–1321. [[CrossRef](#)]
71. Li, C.H.; Cervantes, M.; Springer, D.J.; Boekhout, T.; Ruiz-Vazquez, R.M.; Torres-Martinez, S.R.; Heitman, J.; Lee, S.C. Sporangiospore Size Dimorphism Is Linked to Virulence of *Mucor circinelloides*. *PLoS Path.* **2011**, *7*, 1553–7366. [[CrossRef](#)] [[PubMed](#)]
72. Sayeda, A.A.; Mohsen, S.A.; Osama, H.; Azhar, A.H.; Saher, S.M. Biodiesel production from Egyptian isolate *Fusarium oxysporum* NRC2017. *Bull. Nation. Res. Centre* **2019**, *43*, 210. [[CrossRef](#)]
73. Chang, Y.H.; Chang, K.S.; Lee, C.F.; Hsu, C.L.; Huang, C.W.; Jang, H.D. Microbial lipid production by oleaginous yeast *Cryptococcus* sp. in the batch cultures using corncob hydrolysate as carbon source. *Biomass Bioenergy* **2015**, *72*, 95–103. [[CrossRef](#)]
74. Naveira-Pazos, C.; Veiga, M.C.; Kennes, C. Accumulation of lipids by the oleaginous yeast *Yarrowia lipolytica* grown on carboxylic acids simulating syngas and carbon dioxide fermentation. *Biores. Technol.* **2022**, *360*, 127649. [[CrossRef](#)] [[PubMed](#)]
75. Karim, A.; Islam, M.A.; Yousuf, A.; Khan, M.M.R.; Faizal, C.K.M. Microbial lipid accumulation through bioremediation of palm oil mill wastewater by *Bacillus cereus*. *ACS Sustain. Chem. Eng.* **2019**, *7*, 14500–14508. [[CrossRef](#)]

76. Alvarez, H.M.; Hernández, M.A.; Lanfranconi, M.P.; Silva, R.A.; Villalba, M.S. *Rhodococcus* as biofactories for microbial oil production. *Molecules* **2021**, *26*, 4871. [[CrossRef](#)]
77. Chintagunta, A.D.; Zuccaro, G.; Kumar, M.; Kumar, S.J.; Garlapati, V.K.; Postemsky, P.D.; Kumar, N.S.; Chandel, A.K.; Simal-Gandara, J. Biodiesel production from lignocellulosic biomass using oleaginous microbes: Prospects for integrated biofuel production. *Front. Microbiol.* **2021**, *12*, 658284. [[CrossRef](#)]
78. Shah, A.M.; Mohamed, H.; Zhang, Z.; Song, Y. Isolation, characterization and fatty acid analysis of *Gilbertella persicaria* DSR1: A potential new source of high value single-cell oil. *Biomass Bioenergy* **2021**, *151*, 106156. [[CrossRef](#)]
79. Fazili, A.B.A.; Shah, A.M.; Zan, X.; Naz, T.; Nosheen, S.; Nazir, Y.; Ullah, S.; Zhang, H.; Song, Y. *Mucor circinelloides*: A model organism for oleaginous fungi and its potential applications in bioactive lipid production. *Microb. Cell Factories* **2022**, *21*, 29. [[CrossRef](#)]
80. Karamerou, E.E.; Webb, C. Cultivation modes for microbial oil production using oleaginous yeasts—A review. *Biochem. Eng. J.* **2019**, *151*, 107322. [[CrossRef](#)]
81. Paul, T.; Sinharoy, A.; Baskaran, D.; Pakshirajan, K.; Pugazhenthii, G.; Lens, P.N. Bio-oil production from oleaginous microorganisms using hydrothermal liquefaction: A biorefinery approach. *Crit. Rev. Environ. Sci. Technol.* **2022**, *52*, 356–394. [[CrossRef](#)]
82. Shaigani, P.; Awad, D.; Redai, V.; Fuchs, M.; Haack, M.; Mehlmer, N.; Brueck, T. Oleaginous yeasts-substrate preference and lipid productivity: A view on the performance of microbial lipid producers. *Microb. Cell Factories* **2021**, *20*, 220. [[CrossRef](#)] [[PubMed](#)]
83. Buosi, G.M.; da Silva, E.T.; Spacino, K.; Silva, L.R.C.; Ferreira, B.A.D.; Borsato, D. Oxidative stability of biodiesel from soybean oil: Comparison between synthetic and natural antioxidants. *Fuel* **2016**, *181*, 759–764. [[CrossRef](#)]
84. Bouras, H.D.; Yeddou, A.R.; Bouras, N.; Hellel, D.; Holtz, M.D.; Sabaou, N.; Chergui, A.; Nadjemi, B. Biosorption of Congo red dye by *Aspergillus carbonarius* M333 and *Penicillium glabrum* Pg1: Kinetics, equilibrium and thermodynamic studies. *J. Taiwan Inst. Chem. Eng.* **2017**, *80*, 915–923. [[CrossRef](#)]
85. Singh, G.; Dwivedi, S.K. Mechanistic, adsorption kinetics and confirmatory study of Congo red dye removal by native fungus *Aspergillus niger*. *Biomass Convers. Biorefinery* **2022**, 1–19. [[CrossRef](#)]
86. Zhao, S.; Zhou, T. Biosorption of methylene blue from wastewater by an extraction residue of *Salvia miltiorrhiza* Bge. *Bioresour. Technol.* **2016**, *219*, 330–337. [[CrossRef](#)]
87. Dada, E.O.; Ojo, I.A.; Alade, A.O.; Afolabi, T.J.; Jimoh, M.O.; Dauda, M.O. Biosorption of bromo-based dyes from wastewater using low-cost adsorbents: A review. *J. Sci. Res. Rep.* **2020**, *26*, 34–56. [[CrossRef](#)]
88. Wu, J.; Zhang, Z.; Xu, J.; Lu, X.; Wang, C.; Xu, H.; Yuan, H.; Zhang, J. Brewer's grains with different pretreatments used as bio-adsorbents for the removal of Congo red dye from aqueous solution. *BioResources* **2020**, *15*, 6928–6940. [[CrossRef](#)]
89. El Haddad, M.; Slimani, R.; Mamouni, R.; Laamari, M.R.; Rafqah, S.; Lazar, S. Evaluation of potential capability of calcined bones on the biosorption removal efficiency of safranin ascationic dye from aqueous solutions. *J. Taiwan Inst. Chem. Eng.* **2013**, *44*, 13–18. [[CrossRef](#)]
90. Vairavel, P.; Murty, V.R. Decolorization of Congo red dye in a continuously operated rotating biological contactor reactor. *Desalin. Water Treat* **2020**, *196*, 299–314.
91. Ghoniem, A.A.; Moussa, Z.; Alenzi, A.M.; Alotaibi, A.S.; Fakhry, H.; El-Khateeb, A.Y.; Saber, W.I.; Elsayed, A. *Pseudomonas alcaliphila* NEWG-2 as biosorbent agent for methylene blue dye: Optimization, equilibrium isotherms, and kinetic processes. *Sci. Rep.* **2023**, *13*, 3678. [[CrossRef](#)] [[PubMed](#)]
92. Bagchi, M.; Bera, D.; Adhikari, S. Biosorption of an azo dye Reactive Blue 4 from aqueous solution using dead and CMC immobilized biomass of *Rhizopus oryzae* (MTCC 262). *Bioremediat. J.* **2021**, *25*, 326–346. [[CrossRef](#)]
93. Tran, H.N.; You, S.J.; Hosseini-Bandegharaei, A.; Chao, H.P. Mistakes and inconsistencies regarding adsorption of contaminants from aqueous solutions: A critical review. *Water Res.* **2017**, *120*, 88–116. [[CrossRef](#)]
94. George, G.; Saravanakumar, M.P. Facile synthesis of carbon-coated layered double hydroxide and its comparative characterisation with Zn–Al LDH: Application on crystal violet and malachite green dye adsorption—Isotherm, kinetics and Box-Behnken design. *Environ. Sci. Pollut. Res.* **2018**, *25*, 30236–30254. [[CrossRef](#)]
95. Kumar, R.; Laskar, M.A.; Hewaidy, I.F.; Barakat, M.A. Modified adsorbents for removal of heavy metals from aqueous environment: A review. *Earth Syst. Environ.* **2019**, *3*, 83–93. [[CrossRef](#)]
96. Le, H.Q.; Sekiguchi, Y.; Ardiyanta, D.; Shimoyama, Y. CO<sub>2</sub>—Activated Adsorption: A New Approach to Dye Removal by Chitosan Hydrogel. *ACS Omega* **2018**, *3*, 14103–14110. [[CrossRef](#)]

**Disclaimer/Publisher's Note:** The statements, opinions and data contained in all publications are solely those of the individual author(s) and contributor(s) and not of MDPI and/or the editor(s). MDPI and/or the editor(s) disclaim responsibility for any injury to people or property resulting from any ideas, methods, instructions or products referred to in the content.